WHAT IS THE RELATIVE TIMING BETWEEN MYOSIN'S POWERSTROKE AND PI-RELEASE?

A Dissertation Presented

by

BRENT SCOTT

Submitted to the Graduate School of the
University of Massachusetts Amherst in partial fulfillment
of the requirements for the degree of

DOCTOR OF PHILOSOPHY

May 2022

Kinesiology

WHAT IS THE RELATIVE TIMING BETWEEN MYOSIN'S POWERSTROKE AND PI-RELEASE?

A Dissertation Presented

by

BRENT SCOTT

Approved as to style and content by:

Ned Debold, Chair

Marco Capitanio, Member

Someone else, Member

Someone else, Member

Richard Van Emmerik, Department Chair
Kinesiology

DEDICATION

To Megan, Marilyn, Mollie, and Anna.

ABSTRACT

WHAT IS THE RELATIVE TIMING BETWEEN MYOSIN'S POWERSTROKE AND PI-RELEASE?

MAY 2022

BRENT SCOTT

B.S., BELMONT UNIVERSITY

M.S., UNIVERSITY OF MASSACHUSETTS AMHERST

Ph.D., UNIVERSITY OF MASSACHUSETTS AMHERST

Directed by: Professor Ned Debold

Myosins are a family of motor proteins responsible for various forms of cellular motil- ity, including muscle contraction and vesicular transport. The most fundamental aspect of myosin is its ability to transduce the chemical energy from the hydrolysis of ATP into mechanical work, in the form of force and/or motion. A key unanswered question of the transduction process is the timing of the force-generating powerstroke relative to the release of phosphate (Pi) from the active site. We exam- ined the ability of single-headed myosin Va to generate a powerstroke in a single molecule laser trap assay while maintaining Pi in its active site, by either elevating Pi in solution or by introducing a mutation in myosin's active site (S217A) to slow Pi- release from the active site. Upon binding to the actin filament, WT myosin gener- ated a powerstoke rapidly (500 s-1) and without a detectable delay, both in the absence and presence of 30 mM Pi. The elevated levels of Pi did, however, affect event lifetime, eliminating the longest 25 percent of binding events, confirming that Pi rebound to myosin's

active site and accelerated detachment. The S217A construct also generated a powerstroke similar in size and rate upon binding to actin despite the slower Pi release rate. These findings provide direct evidence that myosin Va generates a powerstroke with Pi still in its active site. Therefore, the findings are most consistent with a model in which the powerstroke occurs prior to the release of Pi from the active site.

TABLE OF CONTENTS

LIST OF TABLES

Table **Page**

LIST OF FIGURES

Figure **Page**

CHAPTER 1

INTRODUCTION

1.1 Historical Significance of the Cross-Bridge to Muscle Physiology and Kinesiology

A fundamental aspect of Kinesiology is centered upon understanding the mechanisms of human motion. Ultimately, every human movement is a direct result of a molecular motor (like myosin) transducing the chemical energy of adenosine triphosphate (ATP) into a mechanical force. Understanding how human skeletal muscle can accomplish the coupling between biochemistry and mechanics has transcended any single field of science over the past century and has required a multi-disciplinary approach to reach the current understanding we currently have on the topic.

In the early 1900s, pioneers in the field of muscle physiology provided the foundational work in understanding how muscles work. During this time the field of biochemistry was unclear of what the exact mechanisms were that provided a muscle cell with the necessary energy for muscle to contract, which was often contributed to oxygen (or at least some form of an oxidative pathway) (Bassett 2002) or to "lactic acid" (Herzog et al. 2015). In 1920, A.V. Hill observed the liberation of heat during isometric tension of an isolated muscle (Hill and Hartree 1920) showing that muscular force can be produced without oxygen. His findings ultimately led him to a Nobel Prize in 1922 ("The Nobel Prize in Physiology or Medicine 1922," n.d.). This finding was detailed further when Wallace Fenn demonstrated that when allowed to shorten, a contracting muscle liberates more heat than when held isometrically (now well known as the Fenn effect) (Fenn 1924). Subsequently, Bailey (1937) characterized

the abundance of myosin in skeletal muscle and Engelhardt and Ljubimowa (1939) demonstrated that myosin was indeed responsible for the muscle's enzymatic activity and consequently the heat production that was observed by Hill and Fenn during their isolated muscle studies years prior. However, despite these early advances there was still no explanation for how a muscle (let alone a myosin molecule) could use ATP to produce force.

The next major breakthrough propelling the field closer to an answer for the mechanism of molecular force production came in 1954 when a pair of Nature articles from Huxley & Hanson and Huxley & Niedergerke independently provided evidence for muscle contraction via the "sliding filament theory" (A. F. Huxley and Niedergerke 1954; H. Huxley and Hanson 1954). Here, the two research groups describe the ability of myosin in the form of thick-filaments to associate with actin filaments causing sarcomere shortening (i.e. contraction) based on structural observations of contracting myofibrils and single muscle fibers. Even so, the sliding filament theory in of itself is not a mechanism of contraction. In 1957, Andrew Huxley provided the first mechanistic hypothesis about how the relative sliding of filaments could occur based upon modeling myosin as a biased Brownian ratchet. This proposal provided the initial groundwork for the modern-day "cross-bridge theory" of muscle contraction (HUXLEY 1957).

After the emergence of these structural perspectives of the actomyosin cross-bridge system biochemists began attempting to align their observations from solution kinetic studies to further explain the structure function relationship of the cross-bridge providing early kinetic schemes of the rates of the various mechanochemical steps/states of the cross-bridge model (Lymn and Taylor 1971). Since the completion of these foundational studies research into the field of muscle physiology has exploded as technology has advanced temporal and spatial limitations of instrumentation providing unprecedented details into muscle myosin structure and function which has provided

a relatively deep understanding (versus the humble origins) of how the cross-bridges cycle from both a biochemical and structural perspective.

1.2 The Modern Cross-Bridge Cycle

The modern cross-bridge cycle is a mechanochemical system which describes the coordination between myosin's enzymatic biochemistry and structural conformations. Different structural conformations are related to certain biochemical states and influence myosin's affinity for the hydrolysis products and actin. As such, the cross-bridge cycle can be modeled as a summary of the current biochemical and structural conformations with a basic model being:

$$^{1)}AM_{post} \implies {}^{2)}M_{pre}\cdot T \implies {}^{3)}M_{pre}\cdot D\cdot P \implies {}^{4)}AM_{pre}\cdot D\cdot P \implies {}^{5)}AM_{post}\cdot D$$

where A is actin, M_{post} is myosin in a post-powerstroke conformation, M_{pre} is myosin in a pre-powerstroke conformation, T is ATP, D is ADP, and P is P_i.
1) Starting in rigor, myosin occupies a post-powerstroke position strongly bound to actin (Geeves and Holmes 1999; Sweeney and Houdusse 2010). 2) The binding of ATP to myosin causes a structural rearrangement in the active site which ultimately opens the upper and lower 50-kDa (Conibear et al. 2003; Holmes et al. 2003) causing both the detachment from actin and resetting of the lever arm into a pre-powerstroke position (Nesmelov et al. 2011; Trivedi et al. 2015) . 3) ATP hydrolysis occurs constraining the myosin in the pre-powerstroke position. 4) When myosin attaches to actin there is a short lived strongly bound/load bearing state where myosin is pre-powerstroke with both hydrolysis products in the actin site (Llinas et al. 2015; Woody et al. 2019) . 5) The final step in the cycle is where myosin undergoes a powerstroke (i.e. lever arm rotation) and P_i-release which leaves the molecule in a

strongly bound post-powerstroke state with solely ADP occupying the active site. Once ADP is released, myosin is left in rigor and the cycle restarts.

1.3 Powerstroke or P_i-Release? a biophysicists "chicken-or-egg" causality dilemma

While there are many details in the modern day cross-bridge cycle that are seemingly clear and well-established, there is a serious point of contention that remains in the literature to this day. The problem resides in the transition between the *3rd* and *4th* step in the model detailed in section *1.2*. In **one** step, **two** key events are taking place - one mechanical and one biochemical. The mechanical powerstroke and biochemical release of P_i are collapsed into this single step without an explicit declaration of the timing or sequence relative to one other. **Both these events are triggered by actin binding, but does the powerstroke precede P_i-release or does P_i-release "gate" the powerstroke?**. This *is* **the dilemma**. Interestingly, the Powerstroke First and P_i-Release First models are *both* well supported in the literature. The divergence from a common mechanochemical scheme has divided the field for several decades and has ultimately limited the progress of fully understanding how myosin is able to transduce chemical energy into mechanical work as the powerstroke and P_i-release steps are key events in the transduction process. Ultimately, not understanding the precise order of the biochemical and mechanical events during the cross-bridge cycle prevents progress into the mechanisms underlying the molecular nature of energy conservation (1st law of thermodynamics) and limits our ability to develop pharmacological interventions to restore function to diseased, mutated, or compromised motors (HCM, DCM, fatigue, etc.). Moreover, in the emerging field of nanotechnology where researchers have been increasingly more interested in controlling biological motors understanding the precise ordering of steps in the transduction is paramount to the success of the field. For example, if you wanted to control myosin

by preventing the powerstroke from occurring (and assuming a P_i-gating model of the cross-bridge) force production could be halted by trapping P_i in the active site. However, this approach would not work in a Powerstroke First model.

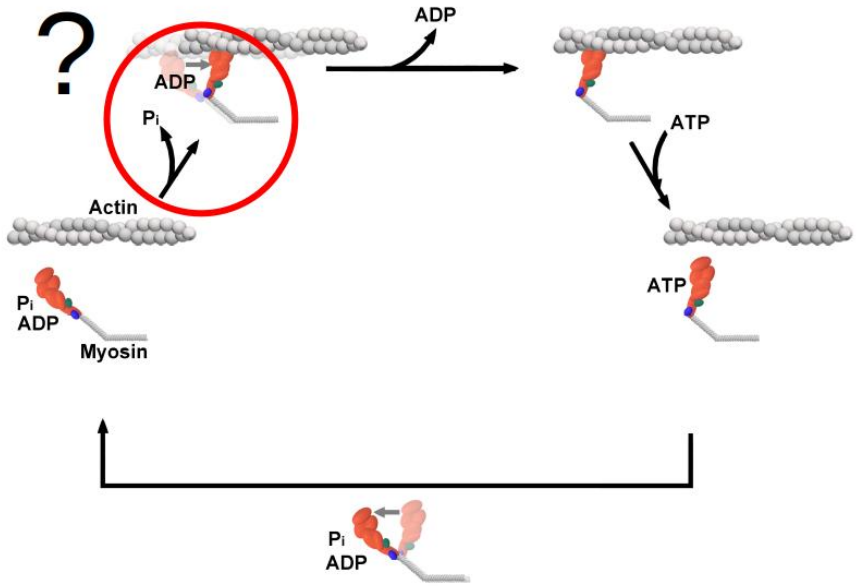

Figure 1.1. A typical model of the cross-bridge cycle. The powerstroke and release of P_i are often represented as ocurring within the same step.

1.4 Q: How can the dilemma be resolved? A: By rigorously testing the current "unifying" theory set forth by structural biologists

In 2015, Llinas et al. (2015) performed x-ray crystallography on phosphate soaked myosin crystals and reported a new and never-before-seen myosin conformation that was posited to provide a unifying theory between the Powerstroke First and P_i-Release First models. This conformational state was aptly named the P_i-Release State (P_iR State). Accompanying the P_iR state, they provided a hypothesis regarding the structural sequence of P_i being released from myosin: 1) Myosin is in a Pre-powerstroke

state (PPS) with P_i in active site, 2) the release of P_i from the active site into the so-called "phosphate release tunnel" causes slight re-arrangement into the P_iR2 state (this is Powerstroke gating in their model), and 3) the final crystal structures detail P_i in the P_iR1 state as the P_i is released into solution from the P_i-release tunnel. The subtly is that there are **two** different P_i-releases. A phosphate can be released from the active site into the P_i-release tunnel as well as be released from the P_i tunnel in myosin out into solution. Moreover, they state that the P_i-release from the active site into the P_i-release tunnel (PPS to P_iR2 transition) is what gates the powerstroke and not the release from the tunnel into solution (see literature review for more details). Now, this is an elegant hypothesis that would explain away some of the most convincing functional data that supports the Powerstroke First model. Mainly, in coupled assays where the force of a muscle fibers is measured simultaneously with the rate of P_i-release (with a phosphate binding protein), or in the case with solution kinetic studies and FRET, the rate of the powerstroke is always measured to be far greater than any measured P_i-release rate. However, with the P_iR state the structural biologists argue that a phosphate binding protein would be binding P_i in solution with the equivalent myosin structural state being P_iR1 or later. Aka, the structural biologists are saying that an assay where a phosphate binding protein is used to measure the rate of P_i-release is actually measuring the wrong rate which makes the previous reports where the powerstroke was found to occur at faster rates an unfair comparison and that indeed the P_iR2 to P_iR1 is rapid and able to gate the powerstroke. However, this current "unifying" theory set forth in recent years remains to be rigorously tested and provides a testable hypothesis - *If the transition of P_i from the active site into the P_iR2 position gates the powerstroke, then can the powerstroke be prevented or slowed by occupying the active site with P_i?*

1.5 Problem: the powerstroke is FAST. How do I see it? Solutions: Build a better mouse trap or get a slower mouse.

While the question is simple, "can the powerstroke be prevented or slowed by occupying the active site with P_i?" devising a way to test this is not so simple for one main reason - the powerstroke occurs quite rapidly upon binding to actin (upwards of 5000/s) (Marco Capitanio et al. 2012; Woody et al. 2019). Being able to assess whether or not experimental conditions can affect the powerstroke is quite challenging. Ideally, these experiments will be conducted in a 3-bead laser trap assay which allows for the observation of single actomyosin binding events and through further analysis the displacement of every individual event can be measured and average displacements can be calculated and compared amongst the conditions. Furthermore, after the identification of the individual events, the trapping records can be ensemble averaged in order to measure the averaged rate of the transition from unbound to bound states. Experimentally, there are two ways that can be used to occupy myosin's active with P_i. 1) By increasing the concentration of free P_i in solution the probability of P_i rebinding into the active site is increased, or 2) by using a mutation that prevents the release of P_i from the active site into the P_i-release tunnel (the S217A mutation in myosin V does just this) (Forgacs et al. 2009; Llinas et al. 2015). Really, the S217A mutation is just a "slower mouse" and affords the ability to use standard trapping techniques in order to test the "unifying" theory. The S217A mutation in myosin V has been shown to have an impaired rate of P_i-release of 30/s Llinas et al. (2015) which is far slower than the WT control myosin V (200/s). An event occurring at 30/s would on average take 33 milliseconds to be completed. If the release of P_i from the active does indeed gate the powerstroke there should be long delays between S217A myosin binding actin and the powerstroke (~33 milliseconds) which would readily be observable under a standard optical trapping setup that has

millisecond time resolution. However, most WT myosins still have a relatively fast P_i-release rate when compared to the resolution of a standard optical trap which might still make the determination of the order of these events difficult. To overcome this, the Ultra-Fast Force Clamp (UFFC) has been used previously which provides sub-millisecond time resolution and allows for the observation of weak binding, an initial force bearing state, and the powerstroke itself in individual actomyosin binding events Woody et al. (2019). More simply, the UFFC is the "better mouse trap."

1.6 Two steps forward, one step back

As presented there is seemingly a couple plausible experiments that can be performed to further assess the "unifying" theory of the powerstroke-first and Pi-release first model. However, there are currently not **any** free open source software (FOSS) projects whose goal is specifically for the automation of single molecule laser trapping data. This (perhaps) is one of the biggest obstacles that is limiting the field of single molecule biophysics. Without a community of software developers there are no standards for the analysis of our data and every new scientist (like myself) has to re-invent the wheel (or at least some version of it) from what they can piece together from the (sometimes *very* minimal) information provided by the methods section of an article. Unfortunately, I have no quantitative evidence supporting the limitations that a lack of analysis software is imposing on the field, but the evidence I do have is personal and anecdotal. This dissertation. As a graduate student I have identified and defended a research topic through my comprehensive exams and have even outlined in previous sections (see 1.4, 1.5) some of the scientific/experimental approaches that could serve as foundation to help progress the knowledge of the field on this given topic. However, even if I was handed all of the data needed to complete the project, I would not be able to answer the questions. Why? Because I do not have the right analysis programs/tools. Generally there are two commons methods for an-

alyzing single molecule laser trap data, 1) single molecule event identification (event picking) and 2) Mean Variance (MV) analysis (see Literature Review for more details on single molecule analysis techniques). Our lab primarily uses MV for analyzing single molecule data (Woodward et al. 2020; Unger and Debold 2019) and has had success with this method. While there are pros to using MV (see Literature Review) it may not be the best candidate to answer my specific questions. Mainly, MV does not identify individual events and as a result additional post-analyses cannot be run on the data, like ensemble averaging. With MV, a change in the magnitude of the displacement of the powerstroke could be estimated, but the rate of this transition could not be determined. This is a key question that needs to be answered for this project to be successful and so an event picking analysis program is needed. But, there are no available programs that implement this, that could be used easily, or that is FOSS. Sure, plenty of research groups have their *own* programs, but the source code is not available and details are limited (some authors do not even mention software/programming languages used) about how specific analyses work which makes replicating an analysis tricky and quite difficult and imposes a serious limitation to the **reproducibility** of work in the field.

1.7 Specific Aims

1.7.1 Aim 1: Develop software to automate the analysis of laser trap data

The current analysis in use by our lab (MV) is not sufficient to answer the questions presented here and answering these questions will ultimately help progress our understanding of how myosin converts chemical energy into mechanical work. An analysis program will be developed that can identify single molecule actomyosin interactions from raw trapping data with the ability to perform ensemble averaging in order to estimate the rate of the powerstroke (transition from unbound to bound). Moreover, the program will have a user-friendly graphical user interface (GUI) and

be free and open source. The analysis will be written in the R programming language (which in of itself is FOSS) and the user interface built with Shiny (an R package that provides a web application framework). With both the analysis program and R language being FOSS, others may contribute/customize the analysis to their needs and improve the operating standards of single molecule trap analysis by offering community developed analysis solution. Additionally, this program will offer a practical, yet advanced, set of tools for other graduate students and research groups to easily implement in their own respective work. "Under the hood" the program will implement the current "best practices" of single molecule event detection by being able to access a robust network of R add-on packages written and developed by experts in their respective field (these R packages of course being well documented and well cited). Lastly, the program should not just be for analyzing single laser trap data records, but should be in fact a complete data analysis and data management tool that will offer easy-to-use tools to perform calibrations, data cleaning and management, analysis, as well as being able to perform project summary statistics. In essence, this program will be a tool that will completely automate the analysis of laser trap data from raw data to final figures.

1.7.2 Aim 2: Test the "slower mouse." Determine if the S217A mutation in myosin V has a reduced displacement or rate of its powerstroke.

S217A is an ideal candidate to test the sequence of events surrounding the timing of the powerstroke and P_i-release in the 3-bead laser trap assay. The main advantage being that S217A effectively traps the -phosphate in the active site which has been shown to have a drastic effect on slowing the P_i-release rate as previously measured in solution kinetics studies (~30/sec). Our hypothesis is that if P_i-release gates the powerstroke, we should observe a prolonged (~33 milliseconds) delay (time period characterized by a decrease in variance of the trapping signal with no displacement)

between the initial binding of myosin to actin and occurrence of the powerstroke. The resulting effects of the S217A mutation would be a reduced displacement (leftward shift in the displacement distribution compared to WT) and a slowed transition rate in the ensemble averaged data. However, if the powerstroke precedes P_i-release then the S217A displacement distributions, and ensemble averages should look identical to the WT. Additionally, performing this same experiment again with high (30mM) P_i in solution will provide an alternative methods for attempting to occupy the active site with P_i. As such, our hypothesis is that if P_i gates the powerstroke there should be a prolonged delay between the initial binding and powerstroke (but much longer in time for S217A vs WT due to slowed P_i-release rate). If the powerstroke precedes P-release then all 4 conditions WT 0mM-P_i, WT 30mM-P_i, S217A 0mM-P_i, and S217A 30-mM-P_i will have identical displacement distributions and ensemble averages.

1.7.3 Aim 3: Test the "better mouse trap." Determine if fast chicken skeletal muscle myosin II has an altered displacement or rate of its powerstroke under high levels of P_i by analyzing data from the UFFC.

While the S217A provides an ideal test since the mutation has drastic affects on slowing the P_i-release rate, there are still limitations imposed by the setup of the standard optical trapping technique that prevent direct observation of myosin binding actin and the subsequent powerstroke. UFFC provides an increased time resolution and allows for the direct observation of the rate of a single powerstroke by a single molecule of myosin interacting with a single actin filament. This is in contrast to inferring an averaged "powerstroke" rate from the ensemble averaged data collected under a standard trapping protocol. Furthermore, the UFFC has the necessary time resolution in order to test a faster myosin isoform (chicken fast skeletal muscle myosin II) under no (0mM) and high (30mM) P_i which will provide additional data on a

different myosin isoform helping to provide a more robust and inclusive answer to the proposed question. Our hypothesis is if P_i-release gates the powerstroke there should be a prolonged initial weak binding state between the binding of myosin to actin and the powerstroke under 30mM P_i compared to 0mM P_i, but the rate of the actual powerstroke should be unchanged.

CHAPTER 2

LITERATURE REVIEW

This review is aimed to be a comprehensive examination of the literature with a scope highly focused on the aspects most fundamental to the main question addressed by this dissertation (what is the relative timing of the powerstroke and P_i-release from myosin?). The review will begin by briefly covering myosin structure and move specifically into how P_i is released from the active site and how lever arm rotation occurs before discussing the evidence in-support of both the Powerstoke First and P_i-Release First models. Additionally, methodological limitations will be addressed here as this may/may not confound the conclusions drawn from a report. Lastly, an evaluation of common analysis techniques of single myosin molecule laser trap will be given including an emphasis on the lack-of availability of user friendly software.

2.1 Myosin Structure

Myosin is a motor protein that accomplishes a wide variety of cellular tasks that includes both muscle contraction (myosin II) and intracellular cargo transport (myosin V). In fact, the myosin (super) family is quite large and has >100 different myosin isoforms (Hodge, Jamie, and Cope 2000) that have traditionally been classified into >30 different structural classes. However, more recently there has been an effort to more quantitatively classify myosins into four groups based on mechanic and kinetic parameters. This grouping schema classifies a myosin as either a 1) fast mover, 2) slow/efficient force holder, 3) strain sensor, and 4) gate (Bloemink and Geeves 2011). Despite a large diversity of job that each myosin performs, they all are mechanochem-

ical enzymes with conserved structures which allows them to transduce the chemical energy of ATP into a mechanical force imposed onto an actin filament. The conserved structures in the myosin motor domain contains 3 distinct sites which interact together allowing the enzymatic (biochemical) and mechanical function of the whole protein to occur. The sites are the 1) active site, 2) the actin binding surface, and 3) the lever arm (Robert-Paganin et al. 2020). Structural changes that occur at both the actin binding surface and in the active site ultimately are communicated throughout the entire protein which effects the position of the lever arm.

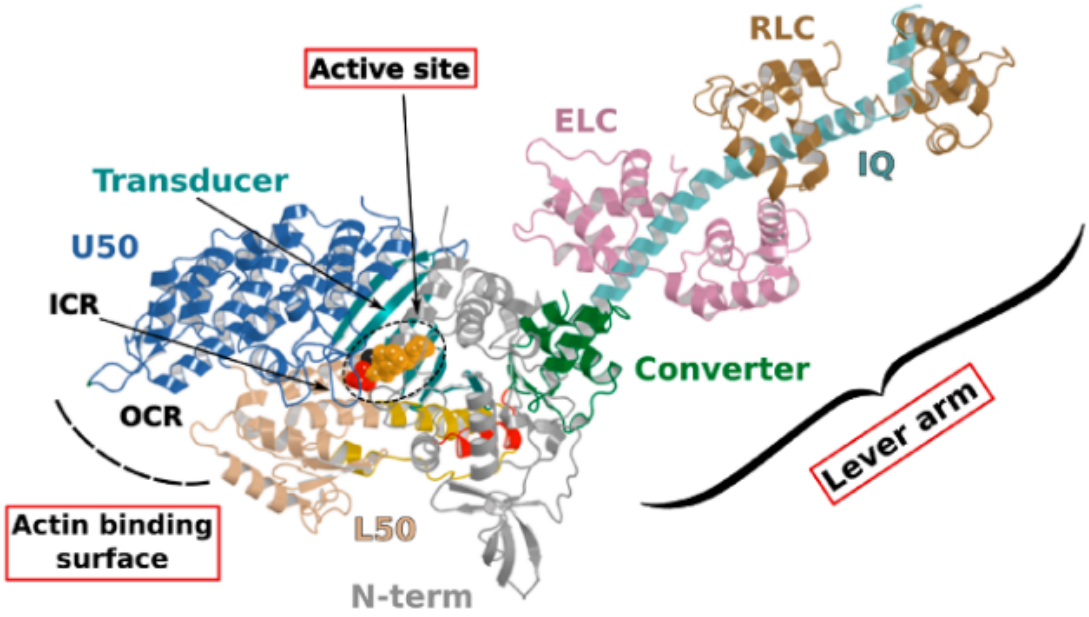

Figure 2.1. Myosin Structure from Robert-Paganin 2020. The three main conserved sites are highlighted in red boxes. ATP is shown in a dashed circle.

2.1.1 How does P_i leave the active site?

When binding to myosin, an ATP molecule enters the active site " -phosphate first." The implications of this is that when ATP is hydrolyzed to ADP + P_i , the ADP molecule blocks the P_i exit pathway the way that ATP entered. Counterintuitively, P_i-

release occurs first prior to the release of ADP in myosin's cross-bridge cycle (Geeves, Goody, and Gutfreund 1984). But, how does P_i leave the active site if ADP is blocking the exit? There are three proposed pathways that lead into myosin's active site and they are nicknamed the "front door," "back door," and "side door." The position of ATP in the active site was first observed when myosin's crystal structure was first resolved (Rayment et al. 1993). At this time solution kinetic studies had established the timing of some of the biochemical steps and was clear that the P_i-release step occurred before the release of ADP. With the observation of ATP in the active site " -phosphate first" it became clear that P_i could not leave the same way it originally entered (via the "front door") due to steric blocking by ADP. With this data the hypothesis was made that myosin could be a "back door" enzyme in which P_i could escape through the 50-kDa cleft (Gilson et al. 1994; Rayment et al. 1993; Yount, Lawson, and Rayment 1995). Additionally, over time other hypotheses arose most prominently with the idea of P_i leaving through a "side door" which forms from an opening in between SWII and the P-loop from the active site. To date, the most probable P_i-release pathway is via the "back door" and is thoroughly detailed by Llinas et al. (2015). Using x-ray crystallography, myosin-VI, varying levels of [P_i] concentrations, and numerous active site point mutations they characterized a so-called "P_i-release tunnel" in between the cleft of the two 50-kDa domains that lead from the active site into solution. In short, the mechanism of P_i-release involves actin binding triggering conformational changes in the active site. SWII opens the entrance to the P_i-release tunnel in which the P_i can dissociate from the active site into solution. Additionally, they were able to couple their structural observations with kinetic solutions studies to show the higher probability of the "back door" mechanism versus the alternate "side door" hypothesis.

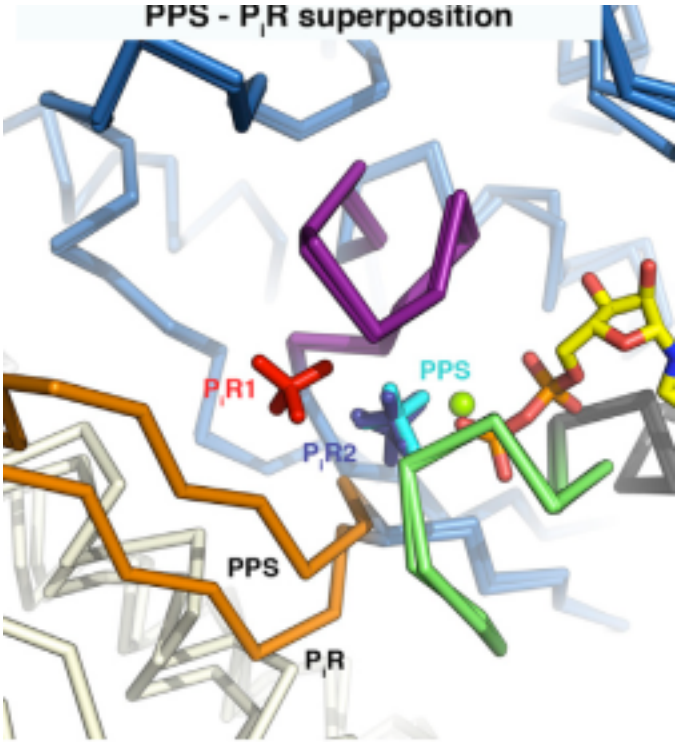

Figure 2.2. The so-called 'P i -release tunnel' detailed by X-Ray Crystallography from Llinas et al. 2015.

2.1.2 How does the powerstroke occur?

Unfortunately, there are no structures of the transition states that occur throughout the cross-bridge cycle and thus there is limited knowledge of the structural rearrangements that occur during the main part of the powerstroke (the force generating step), however what is known is that there is a large lever arm rotation between the initial force bearing P_iR state and the strongly bound ADP state that is coupled with cleft closure (Sweeney, Houdusse, and Robert-Paganin 2020). Structural data has however provided information about the size of the lever arm, ~9nm in chicken skeletal S1 (Rayment et al. 1993), which is in close proximity with single molecule displacement records measured in the laser trap, 5-10nm, for skeletal myosins containing two IQ domains Tanaka et al. (1998). In addition, the displacement of the powerstroke scales with the length of the lever arm which is dependent on the number of IQ domains (Matthew J. Tyska and Warshaw 2002). In comparison, myosin V S1 that contains 6 IQ domains was measured to have an average displacement ~18 nm (Veigel et al. 2002). Interestingly, the displacement of myosin V S1 is about three times larger than that of myosin II S1 as myosin V S1 also contains three times the number of IQ domains.

Along with the length measurements, estimations of the degrees of rotation of the lever arm have been made. Several groups have estimated a large 65-75 degree rotation of the lever arm which occurs as result of the powerstroke (Dominguez et al. 1998; Houdusse, Szent-Györgyi, and Cohen 2000; Walker et al. 2000). Admittedly, though the estimations of the displacement caused by the powerstroke are rather close between measurements of the lever arm from structural biologists and displacement records provided by single molecule trappers, there has been speculation on why the displacement measured in the laser trap is often a few nanometers less than predicted by a 9nm lever arm rotating through 70 degrees of motion (this should be >9nm based of structural predictions though many trappers report 5-6nm). Matthew J. Tyska and

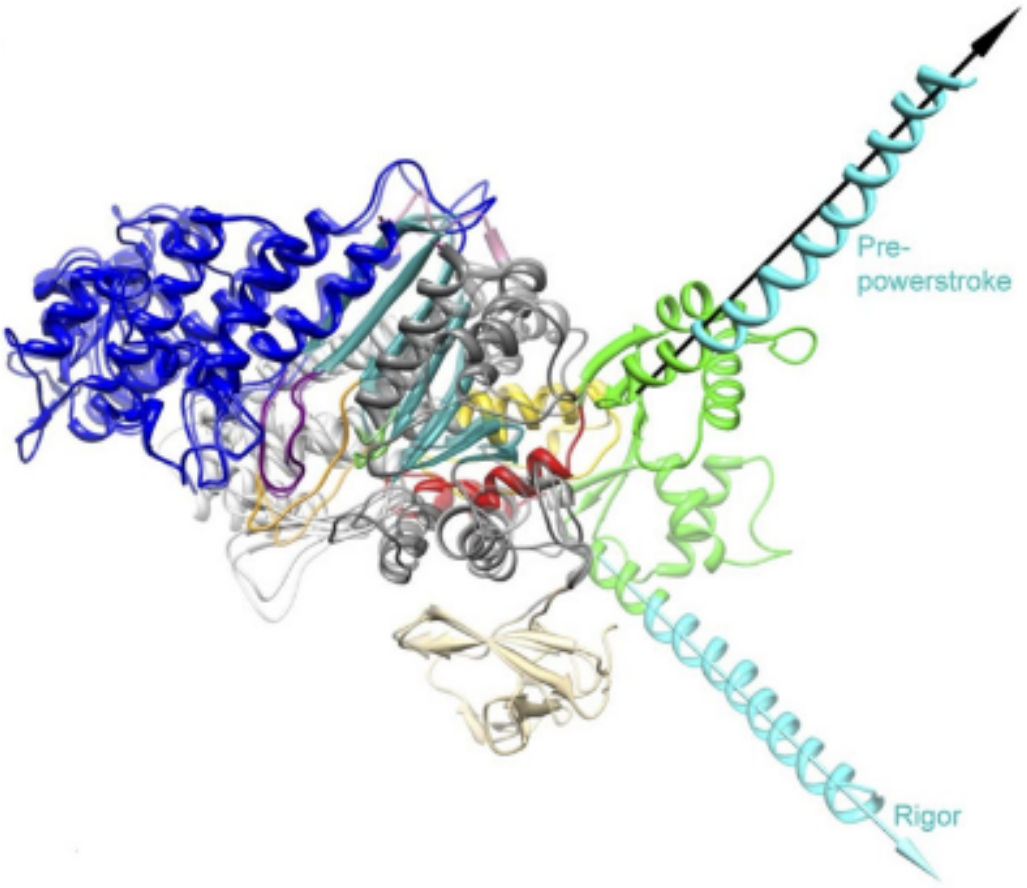

Figure 2.3. Overlayed structures of myosin V in the pre-powerstroke and rigor state from Wulf 2015

Warshaw (2002) attribute the underestimation from trapping studies to the fact that myosin is working against a load in the laser trap. Alternatively, there could also be series compliance that effects the functionally measured displacement in the trap. Furthermore, one of the most notable and important features of the myosin motor domain is the converter. The converter is able to amplify small conformational changes that occur at the actin binding interface and the active site into large movements and re-positioning of the lever arm. The converter is highly flexible and the majority of the series compliance in the myosin has been attributed to this feature (Köhler et al. 2002). Though the lever arm has been suggested to be compliant by some (Howard and Spudich 1996), more recent evidence suggest the lever arm is in fact rigid (Warshaw et al. 2000) since the observation that showed myosins displacement is directly proportional to lever arm length (Matthew J. Tyska and Warshaw 2002). Interestingly, the powerstroke actually occurs in two transitions, the fast powerstroke and the second powerstroke (sometimes referred to as the hitch). The additional lever arm rotation is accompanied by complete closure of the actin binding cleft that is coupled with the release of ADP from the active site (Mentes et al. 2018; Sweeney, Houdusse, and Robert-Paganin 2020). While, the second powerstroke does not contribute much to the development of force, it is crucial to the *maintenance* of force. Changing the rate at which ADP is released from the active site can drastically alter myosin's duty ratio and is highly load dependent. In fact, kinetic differences, including differing ADP release rates, is what make different myosins ideal at performing specific tasks. Through their kinetics myosins as are essentially "tuned" to their biological function. While skeletal muscle myosin II has a low duty ratio (~5%) which makes it ideal for the development of high forces and velocities, myosin V has a much higher duty ratio which allows for one head to always be strongly bound to an actin filament track ensuring the molecule does not simply diffuse off of its actin track.

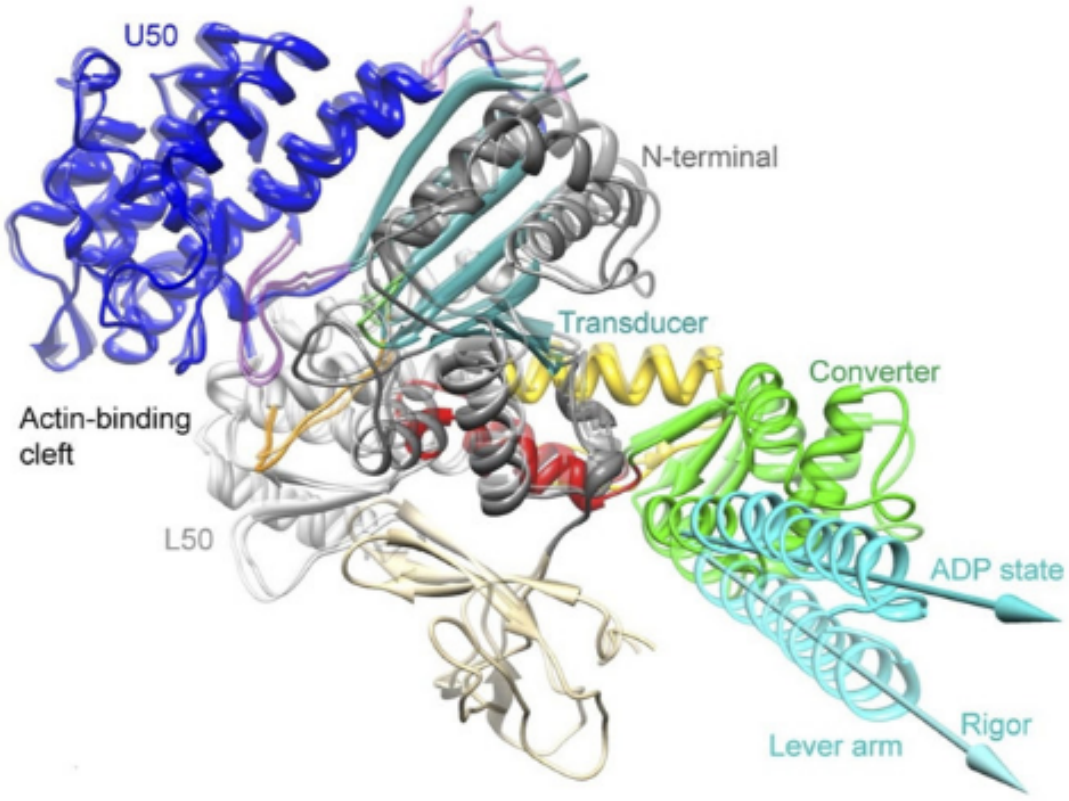

Figure 2.4. Additional lever arm rotation with ADP Release from Wulf 2015

Lastly, the key activator of the myosin powerstroke that is universally agreed upon is actin binding. Really, to try and explain what happens after actin binding would be jumping too far into the major debate happening in the field and is exactly the motivation behind this dissertation. Up until now, what is fairly certainly known (and what is actually generally agreed upon) is that the powerstroke is 1) actin-activated and 2) occurs between an initial force bearing state and the strongly bound ADP state. The details and order of events that occur has been debated for years and the answer to the question "how does the powerstroke occur?" is highly dependent on who is asked. Two distinct and opposing answers are provided by structural biology and the results of functional experiments.

2.2 The Debate

The relative timing of the powerstroke and P_i-release is the big question in the myosin world. This question has been tested and re-tested and evidence continues to build for *each* side. The perspective from structural biologists holds the view that **P_i-release gates the powerstroke** and *they have the data to back it up.* However, functional assays performed by muscle physiologists, biochemists, and biophysists support the idea that the **powerstroke occurs prior to P_i-release** and that actin-binding alone is enough to trigger the powerstroke, and *they have the data to back it up.*

2.2.1 Evidence for the Powerstroke Preceding P_i-release

In a model where myosin's powerstroke occurs before P_i-release there must be a couple of key functional observations that can be observed experimentally in order to support this theory. 1) The development of force or the rate of the powerstroke should be relatively faster than the measured P_i-release rate. 2) The powerstroke should be reversible and/or force production should be vulnerable to P_i rebinding as this should

either reset the myosin to an M_{pre}-D-P state and/or induce premature detachment. Early studies with muscle fibers show isometric tension is inversely proportional to $[P_i]$ - the higher the $[P_i]$ in solution, the lower the force (Brandt et al. 1982). Additionally, the release of caged P_i in isometrically contracting muscle fibers displays a delayed but clear depression in tension (Dantzig et al. 1992). Furthermore, a linked assay that assesses the development of muscle fiber force and the simultaneous appearance of P_i in solution proves that fiber force develops faster than the appearance of P_i in solution (He et al. 1997). Later studies show that the rate of force production following a shortening-restretch protocol is rapid and similar to the original time course of the force development from isometric tension (Sleep, Irving, and Burton 2005). These cellular level studies are clear that a muscle can produce force faster than the release of P_i and that the force developed by a muscle can be affected by P_i rebinding, all in support of a model where the powerstroke occurs before P_i-release. More recently, in vitro investigations using time resolved FRET with fast skeletal myosin II provided direct evidence that the powerstroke proceeds P_i-release by obtaining fluorescence measurements of both the rate of the powerstroke and P_i-release for direct comparison. The rate of P_i-release was measured at 30-40 s-1 and the adoption of a post-powerstroke configuration (i.e. M* Mole Fraction) occurred at 350 s-1 (Muretta et al. 2015). Thus, when directly measured the rate of transition from pre-post powerstroke is far greater than the rate of the appearance of P_i in solution. This finding was corroborated with traditional FRET studies of myosin-V comparing lever arm rotation rate to another independently acquired P_i-release rate (Trivedi et al. 2015). Lastly, ultra-fast optical trapping can directly measure the rate of the powerstroke from a single molecule of myosin (Marco Capitanio et al. 2012). Woody et al. (2019) measured the rate of the powerstroke under varying $[P_i]$ concentrations and saw rapid displacements occurring within ~200us of actin binding and that the dwell time prior to the displacement was unaffected by $[P_i]$. Even so, by

using an ensemble averaging technique they show direct observation of powerstroke reversals (under high loads and high [P_i]) which provides single molecule evidence of the powerstroke proceeding P_i-release.

2.2.2 Evidence for P_i-release Gating the Powerstroke

If P_i-release gates the powerstroke, distinct structural conformations of myosin should exist in order to support this model. 1) When P_i is in the active site myosin should be in a pre-powerstroke position and 2) the adoption of a post-powerstroke configuration should only occur if P_i is absent from the active site. Interestingly, the hypothesis that the biochemical release of P_i from myosin's active site proceeding the powerstroke originally came as a result of first x-ray crystallization of myosin (Rayment et al. 1993) and the subsequent attempts to dock an ATP molecule into the crystal structure since the original myosin structure was crystallized without a ligand. The realization occurred after these efforts that myosin may perhaps be a "back door" enzyme (Yount, Lawson, and Rayment 1995). By extending the "back door" analogy, Yount, Lawson, and Rayment (1995) described P_i as behaving as a "door stop" as it was hypothesized that P_i itself actually prevented the powerstroke from occurring since the P_i appeared to be in a position that would prevent cleft closure (and the subsequent triggering of structural changes necessary for lever arm rotation). Indeed, for over a decade from the original structural characterization of myosin there persisted discrepancies amongst multiple hypotheses about how actin binding could possibly cause the conformational changes necessary in the active site to open the back door (Sweeney and Houdusse 2010). The two possibilities being that either SWI can create the opening for the back door whilst remaining coordinated with the ADP or SWII must somehow open the back door without permitting lever arm rotation. Llinas et al. (2015) provided new myosin x-ray crystallography structures in which they show the ability of SWII to move ~4A from its position in the pre-powerstroke

position, opening the back door escape route without substantial movement of the lever arm. This new state was aptly named the P_i-release state, P_iR. By using a P_i-soaking protocol followed by rapid freezing and subsequent crystallization, Llinas et al. (2015) demonstrated that P_i can translocate back through the P_i-release tunnel as they observed two distinct structural states in response to the rapid freezing after P_i-soaking. P_i was either at the exit of the P_i-release tunnel (P_iR1) or translocated back through the tunnel near the ADP (P_iR2). Only in response to a delayed freezing after P_i-soaking did they observe P_i completely rebinding the active site, consequently reforming the pre-powerstroke state. Thus, they provide strong evidence for P_i-release occurring before the powerstroke - when P_i is in the active site, myosin is in the pre-powerstroke state. Furthermore, when P_i-soaking post-powerstroke myosin in an ADP state, the crystal structures show that the P_i was not able to translocate back through the P_i-release tunnel to the active site. This demonstrated that myosin only adopts a post-powerstroke conformation when P_i is absent from the active site and also that P_i-rebinding can only occur prior to the powerstroke (Llinas et al. 2015). These observations are all consistent with a model in which P_i-release gates the powerstroke.

2.3 Methodological Limitations

As the brief review provided by the previous two sections highlights, there is overwhelmingly strong evidence supporting both models that describe the relative timing of the P_i-release and the powerstroke. Because of this, careful consideration about the methodical and analytical limitations should be understood if there will be any hopes of somehow reconciling the differences observed in the data. To start, the most obvious difference that is evident amongst the data is that the majority of the studies that support the powerstroke first model are all functional assays, whereas the evidence supporting the P_i gating model are largely structural. In essence, structural data provides "snapshots" analogous to the creation of a stop motion film,

whereas the functional studies provide the soundtrack to the movie. We have the two essential pieces to creation of a blockbuster film, but not the information to correctly align the audio to the video. Understanding every detail of these experiments is difficult as the collection methods and analytical techniques for each respective method are the results of multidisciplinary approaches that provide deep knowledge of biology, chemistry, physics, mathematics, and computer science. However, new information can be revealed when the data is put into context of understanding what a measurement is precisely assessing from a given experiment and what factors should be considered when weighing the values in combination in the efforts to generate any given model.

2.3.1 Structural limitations

For example, while the results of x-ray crystallography produce a single structure of a myosin molecule these structures in fact represent the average bias of thousands of molecules (Sweeney and Houdusse 2010). In addition, formation of myosin crystals is extremely difficult and numerous modifications have to be performed on the myosin (i.e. reductive methylation, removal of the heterogeneity in light chain species and varying levels of phosphorylation) to obtain high quality crystals (Rayment et al. 1993). Furthermore, an actin-bound myosin structure is yet to be resolved. Considering the strong evidence that the cross-bridge cycle is actin activated (i.e. accelerated powerstroke and P_i-release rates in the presence of actin (Lymn 1974)), this is an important limitation to be considered (and perhaps the biggest). Lastly, myosin's kinetics are influenced by many factors including load, pH, ionic strength, and $[P_i]$. It is not currently possible to variably apply loads (besides those arise from crystal packing forces) to myosin in x-ray crystallography or electron-microscopy and the solution buffers often have fixed pH and salt concentrations that optimize the formation of crystals and that are not necessarily preferential for myosin's kinetics.

2.3.2 Functional limitations & the "unifying" hypothesis

Now, the functional assays are not without faults of their own. To start, muscle fiber studies, ATPase, stopped-flow, and FRET are all bulk assays. These assays are measuring the average response of thousands of molecules of myosin into a single measurement of the development in tension, powerstroke rate, or P_i-release rate. Even optical trapping measurements of the powerstroke rate from a single molecule of myosin is not as straightforward as it might sound (ask me how I know) and involves an ensemble averaging technique (Blackwell et al. 2021; M. Capitanio et al. 2006; Sellers and Veigel 2010; Veigel et al. 1999, 2003). Moreover, in the trap single molecule displacements are the summation of the distance produced by myosin's powerstroke and that of brownian capture (additional distance caused by thermal noise) and the transition rate going from a pre- to post-powerstroke (i.e. unbound to bound) in the trap is limited by the viscous drag forces imposed by the solution onto the trapping beads (König 2000; Svoboda and Block 1994). As a result, the rate of the powerstroke is often underestimated due to imperfect alignment of single molecule events in the ensemble averages and also in part to the transition rate between unbound/bound periods being similar to the trapping system's corner frequency. In the case of the coupled assays where attempts are made to simultaneously measure the rate of force development in fibers while also recording the P_i-release rate, assessments must be made about the relative time resolution between the two coupled measurements to assure there is a fair comparison between the two respective rates. To this regard comes one of the biggest flaws within the powerstroke first argument. The most current argument put forward by structural biologists who support a P_i-gating model claim that the P_i-release rate measured by muscle fibers and with stopped flow is simply the wrong rate. When Llinas et al. (2015) provided new structural evidence of the P_iR state, they also hypothesized the structural sequence of P_i being released: 1) Pre-powerstroke state (P_i in active site), 2) P_iR2 (P_i transitions from

active site into putative P_i-release tunnel, and 3) P_iR1 (P_i at exit of P_i-release tunnel in solution). A phosphate binding protein binds P_i in solution with the equivalent structural state being P_iR1 or later. Moreover, the structural biologists argue that the P_i transitioning from the active site in the pre-powerstroke state to the P_iR2 state is what actually gates the powerstroke - not the transition into the P_iR1 state - and that the PPS-P_iR2 transition would occur very rapidly. This was proposed to provide a unifying theory between the structural and functional assays that bridges the gap between the powerstroke first and P_i-gating models. *However, this hypothesis remains to be rigorously tested and provides a testable hypothesis - If the transition of P_i from the active site into the P_iR2 position gates the powerstroke, then can the powerstroke be prevented by occupying the active site with P_i?*

2.4 The S217A mutation in myosin V

Several key amino acids in the active site have been identified to interact with the ATP and more specifically, the -phosphate while in the active site (Forgacs et al. 2009; Gulick et al. 2000; Llinas et al. 2015; C. A. Smith and Rayment 1996). Moreover, previous simulations of P_i leaving the active site via the different proposed escape routes highlight important contacts between certain amino acid residues with this fleeting P_i along each proposed route (Cecchini, Alexeev, and Karplus 2010; Reubold et al. 2003). By manipulating the charge or size of these amino acids along the different escape routes with point mutations several research groups have tested whether they could slow the measured release of P_i with a stopped flow assay (Forgacs et al. 2009; Llinas et al. 2015). Serine 217 (S217) was shown to make contact with the -phosphate in the active site from its location on SWI and the S217A mutation drastically reduced the P_i-release rate ~10-fold (Forgacs et al. 2009). With this mutation, S217 was identified as playing an important role in P_i-release. Llinas et al. (2015) verified that the S217A mutation drastically slows P_i-release

and in addition showed S217 mediates the transition of the P_i from the active site into the "P_i-release tunnel" via the back door mechanism with x-ray crystallography. Furthermore, the underlying mechanism of the S217A mutation that slows P_i-release was suggested to be due to the mutation preventing the P_i from transitioning into the P_i-release tunnel via the back door escape route, possible due to a steric blocking by a water molecule or loss of interaction that "guides" the P_i into the release tunnel (Forgacs et al. 2009). Comparatively, the E146A mutation proposed to contact the -phosphate via the alternative side door mechanism (via a SWI movement) had no effect on the P_i release rate (Cecchini, Alexeev, and Karplus 2010; Llinas et al. 2015) which was an observations that led to them supporting the back door mechanism which is currently the prevailing P_i-release pathway hypothesis (Robert-Paganin et al. 2020). Most importantly the S217A mutation provides the perfect test of the "unifying" theory proposed by the structural biologists. The unifying theory states that the transition from the active site into the P_i-release tunnel gates the powerstroke (not the release into solution). With the S217A mutation, we have a mutation that prevents the release of P_i from the active site into the P_i-release tunnel. So, if the release of P_i from the active site into the escape tunnel does gate the powerstroke then the powerstroke should be delayed or prevented with the S217A mutation in myosin V. Furthermore, since the P_i-release rate becomes so much slower (~30/s) the observation of a delayed stroke would be obvious in a standard three-bead laser trap assay which has millisecond resolution. Additionally, myosin V has a much slower and rate limiting ADP-release rate which results in an increased attachment time when compared to fast skeletal myosin II making the attachment events in the laser trap more easily identifiable at high ATP concentrations.

2.5 Analysis of single molecule trap data

> "…the interpretation of data from such experiments [the laser trap] is not straightforward" - Guilford et al. 1997

The laser trap (or optical tweezers) has been revolutionary to the myosin world. Originally developed by Arthur Ashkin of Bell Laboratories (Ashkin et al. 1986) the laser trap was adopted by biologists to study the interactions of a single molecule of myosin with a single actin filament. After the first single molecule three-bead assay was performed in 1994 by Finer, Simmons, and Spudich (Finer, Simmons, and Spudich 1994), single molecule myosin biophysics began to flourish as other research groups began building their own laser traps to investigate the basic mechanical and kinetic properties of the myosin family. While quick to adopt the method of the three-bead assay, the analysis of single molecule laser trap data seemed to be controversial even since the original Finer, Simmons, and Spudich (1994) experiment. Most of the major research groups that were trapping with myosin in the 1990s seemed to have their own opinions on how to best extract the necessary information from their raw data records and several analysis methods seemed popular while other were abandoned or seemingly ostracized by the community. Even the original work of Finer, Simmons, and Spudich (1994) came under scrutiny relatively quickly by the newly found field since they analyzed their data "by eye," manually selecting where actomyosin interactions occurred in the data. Moreover, even more recently as analysis has moved more hands-off and has become increasingly more automated with computer programs, many fail to cite properly (or even explain) the basic underlying programming languages, software, or libraries used to construct their custom analysis scripts (and there is currently no GUI software that is easily accessible to perform the analysis of laser trap data). This makes reproducible research quite difficult, and not just from the point of wanting to replicate someone else's experiments, but also since many reviewers of journal manuscripts expect to see laser trap data analyzed just as "someone else" has done. The lack of software is a large gap in the field and ultimately provides a hindrance to the field progressing as a whole. Following is a review, attempted at being chronological as best as possible, of the (mostly early) trapping

papers and their techniques used to analysis single molecule myosin data from the three-bead laser trap. The purpose is to review what has and is currently being done to analyze single molecule trapping data in hopes highlight the "best practices" that should be included (or would be desired) in a modern software package.

2.5.1 Manual identification

The most simple and easiest way to analyze laser trap data is just to look at it. Manual event identification (the "by-eye" technique) was the original analysis method used by Finer, Simmons, and Spudich (1994). Here, they defined several criteria that would define their "event population" (actomyosin interactions) and would scan through the data record manually marking where they believed each event would start and end. The criteria they used were that 1) events needed to be isolated events with baseline returning to approximately the same "zero" or reference position on each side of the event, 2) the displacements could not have multiple interactions (what most people now called "runs" in mini-ensemble data), and 3) displacements smaller than or equal to the variance of the baseline would not be included.

The reason analysis techniques can be controversial in the field is because many times the information provided by the data and what conclusions can be drawn are in part limited by the analysis performed. For instance, major motivation of the original three-bead assay was to provide a direct measurement of single molecule myosin displacements since there was a large discrepancy from displacement estimations provided by bulk in vitro assays (motility and fibers). Additionally, the first myosin crystal structure had just been solved a year prior by Rayment et al. (1993) which had put structural constraints on myosin's displcament to be ~6nm. However, Finer, Simmons, and Spudich (1994) directly measured a powerstroke that was about twice as large. Why? Their analysis technique was flawed. While Finer, Simmons, and Spudich should no doubt be applauded for their pioneering work, the manu-

ally identification of events caused an over-estimation of their estimate of myosin's displacement (and to be fair hindsight is 20:20 and you have to start somewhere). Ultimately, what occurred is that their inclusion criteria that they defined specified events that needed to exceed the level of the baseline noise of the trapping system, or to be greater in magnitude than the variance of the baseline. Consequently, the analysis then only included the largest displacement events that occurred effectively filtering out the smaller displacements. We now know single molecule displacement events should be normally distributed with a mean equal to the average displacement and variance equal to that of the baseline signal (J. E. Molloy et al. 1995a), Finer, Simmons, and Spudich (1994) essentially truncated their distribution and inflated their mean displacement value. So yes, analysis is important.

Even so, the analysis of trap data continued to hinder the field in their ability to accurately measure the displacement caused by myosin's lever arm that matched those estimation provided by structural biologists. Two years later Molloy et al. 1995 (Biophysics) measured S1 and HMM displacements to be ~15nm. The analysis was similar to Finer et al. 1994, yet J. E. Molloy et al. (1995b) seemed more definitive about setting displacement and time (>10ms) thresholds for the inclusion of events. This method has become commonplace for use with mini-ensemble data where events must be greater than a given displacement threshold for a minimum duration to be considered into the "event population." Interestingly, Molloy et al. 1995 (Biophysics) admits in their own paper that "longer displacements could arise because both their [Finer 1994] and our data events were analyzed by eye; this may have introduced observer bias."

2.5.2 Variance threshold

Another Molloy et al. 1995 (Nature) paper was subsequently released with a new set of trapping data that was analyzed with a variance threshold (the first instance of

a variance based analysis). Previous trapping papers solely used the raw displacement record to identify attachment events, but the introduction of the variance threshold was clever and forms of this are still in wide use today in analysis programs. The principle behind the variance threshold is theoretically simple and practically robust. A small bead trapped by a laser will provide a "noisy" baseline signal that is characterized by Brownian motion. On our trap in the Debold lab, trapping at a laser power of 1.5 Watts usually produces an approximate laser trap stiffness of 0.04 pN/nm. This stiffness value (0.04 pN/nm) is far less than the stiffness of a myosin head. Consequently, as the bead-actin-bead assembly is pushed around by Brownian forces the dumbbell can travel up to ~40nm in either direction (~80nm total excursion distance). However, since a myosin head is far stiffer than trapping laser, when myosin binds to actin there is a large reduction in the variance in the signal and the bead experiences less overall excursion. While, comparing the variance of the unbound to bound population can hard to resolve by eye transforming the original raw displacement records into running variance records makes the difference in bound/unbound variance become more readily apparent as this variance signal-to-noise ratio can exceed a 2:1 ratio (usually at least >4:1 if you are Chris Marang). With the variance threshold analysis J. E. Molloy et al. (1995a) were able to identify zero and low displacement events that would have been excluded from previous analyses. Including zero and low displacement events produced a more complete data distribution to perform summary statistics on which provided a more accurate representation of the true underlying mean that was being estimated from the sample. Ultimately, they were able to conclude that previous measurements of the powerstroke displacement were overestimated due to flawed analysis which produced an incomplete distribution to be collected and biased the final average.

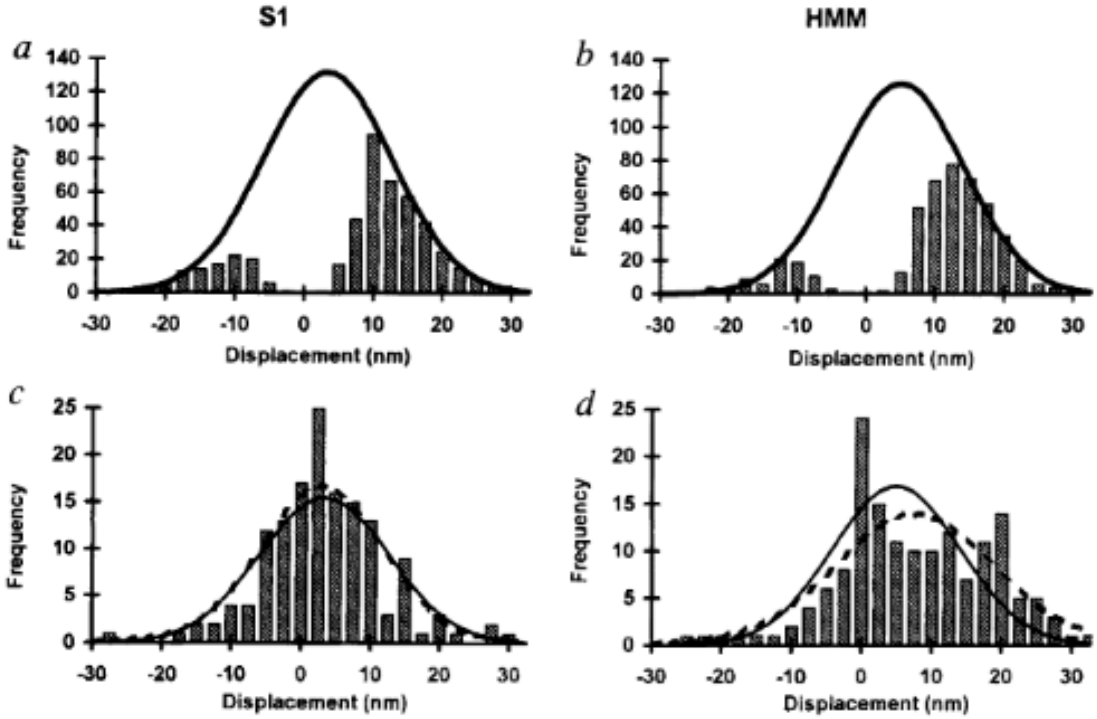

While great strides were made with the variance threshold implementation of J. E. Molloy et al. (1995a) a few issues have persisted since. For one, a clear rationale for the criteria that is used to define a threshold was never really provided leaving one to think this may be arbitrarily set and left to the analyzers discretion as they seek to optimize event identification "by eye" through manipulation of the threshold. Also, no methodological details are provided about how this analysis was performed in regards to software or programming languages. Both of these cause major issues when attempting to reproduce the analysis they argue as superior. Furthermore, this paper becomes heavily cited throughout future research papers conducted by these same authors that end in high impact journals setting the precedent for what is expected from the analysis of laser trap data. Veigel et al. (2002) is in Nature Cell Biology (impact factor ~20 now in the year 2021), has been cited 425 times, and only provides a minimal explanation of the analysis performed and instead simply opts to cite J. E. Molloy et al. (1995a) as reference for their analysis methods which also has an air of ambiguity around the analysis methods.

2.5.3 Correlated thermal diffusion

The first few years of myosin laser trapping mostly used one quadrant photodiode (QPD) to track the position of one of the trapped beads of the bead-actin-bead dumbbell. Mehta, Finer, and Spudich (1997) implemented a two QPD setup where they simultaneously could track the position of both beads. With this additional data they implemented an analysis method they called "correlated thermal diffusion." Since a bead-actin-bead assemble is a rigid system when the setup is unbound from myosin the beads move in unison. As in, the position of one bead is correlated with the other one as they are pushed around by Brownian forces (linked together by a pre-tensioned actin filament). However, when the stiffer myosin head interacts with the actin filament the beads become "disconnected" (figuratively not literally…though, I guess, literally disconnecting is possible, but a separate issue…just use a lot of biotin and then you do not really have to worry about any literal disconnection). As a result, the position of the two trapped beads becomes uncorrelated. Practically, the correlated thermal diffusion analysis can be performed by iteratively applying linear regressions over small windows (data subsets) of the raw displacement data from the two traps and returning the correlation coefficient of the fit. The "event population" will be the transient periods in time when the correlation coefficient drops to zero. The main advantage of correlated thermal diffusion is that the variance signal-to-noise ratio does not have to be as high as in the variance threshold analysis which is usually dependent on the amount of pre-tension that can be applied to the bead-actin-bead assembly and the "stickiness" of the beads. This analysis is quite similar to the covariance analysis method that also utilizes the advantages of having two QPDs, but instead calculates the covariance of the two beads position instead of extracting correlation coefficients from linear regression fits. Since covariance analysis requires two QPDs and our setup only has one, it is not a viable analysis option and will not be included in this review in detail.

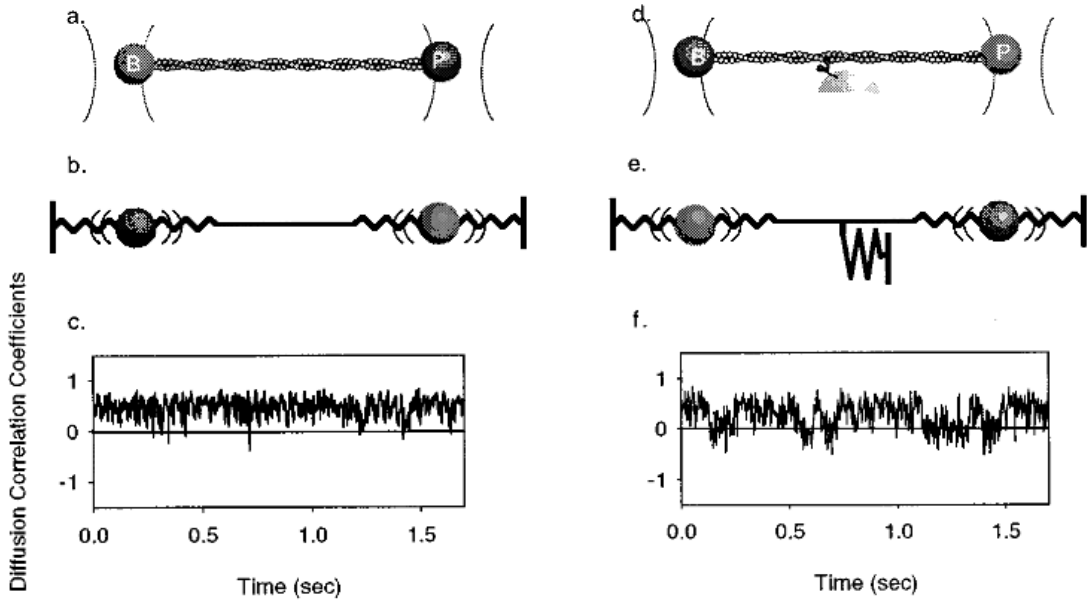

Figure 2.5. Diagrammatic explanation of the correlated thermal diffusion analysis from Mehta et al. 1997.

2.5.4 Mean Variance Analysis

While the original motivation of using the single molecule laser trap was to measure the displacement a single myosin molecule could generate, the first few years produced a discrepancy of displacement estimations that were largely analysis based due to the "eye-balling" of arbitrarily thresholded data. Guilford et al. (1997) (Warshaw Lab at the University of Vermont) re-purposed an analysis technique originally used for single ion channel data to perform the analysis of their single molecule trapping data called "mean variance analysis," or MV (Patlak (1993), both research groups are from the University of Vermont). This technique is a completely different approach than any of the previous attempts at analyzing laser trap data (with myosin as the motor) and extracting displacement data from. Implementation of MV in the laser trap was in response to the previous attempts of estimating myosin's displacement which were made by manually selecting binding events from thresholded data (Finer, Simmons, and Spudich 1994; J. E. Molloy et al. 1995b), a practice that was sub-

sequently shown to be not of "best-practice" as it was not statistically defense-able (Block and Svoboda 1995). The benefits of MV is that it provides a model independent transformation of the data, requires no manual selection/scoring of events by eye, and requires no assumptions about the underlying data. However, the procedure of performing analysis is more complex.

Mean-variance analysis is performed, and so aptly named, by transforming raw trapping data (displacement vs. time) into mean-variance histograms. The MV histograms are 3-dimensional histograms that are constructed by calculating the mean and variance of a "window" (small subset of data). While, the direct results of calculating these windows values results in two time series data set, these can be plotted against each other to construct a 3-dimensional histogram where mean is on the x-axis, variance is on the y-axis, and the "third" z-axis is counts/number of windows/data points and reflects the total time spent at any given mean-variance combination. Since the baseline data (myosin unattached from actin) is characterized by Brownian motion the result of a histogram has a prominent normally distributed "baseline" population with mean centered around zero. If any actomyosin interactions are in the data traces they will present as an alternate "event" population with mean value equal to myosin's displacement size. Additionally, the "event" population will have a smaller variance than the baseline due to myosin being stiffer than the trap. The "event" and "baseline" population can be separated by their variance, typically a data trace that contain no actomyosin binding event is used to "remove" the baseline from the data with events. After, the removal of the "baseline" population the "event" population can be fit by a sum of gaussians to estimate myosin's displacement.

Furthermore, Patlak (1993) showed that average attachment times and the number of events could be estimated with the MV approach. In MV, since the "third" (z-axis) represents the counts/amount of time spent at a given mean-variance this "time" is dependent on the window width used to construct the MV histogram (smaller win-

dows width produce a data set with more data points). By iteratively constructing MV histograms and recording the number of "counts" in the event population, a plot of counts vs window width can be constructed and this relationship is defined by a single exponential. Fitting the exponential $V_{mv} = t_{on}ke^{(N-1)t_{on}}$, provides estimates of the average attachment time (ton) and number of events (k) present in the data which are parameters of the fit.

While thresholding and identifying events "by-eye" is simple, it is also (relatively) easy requiring no sophisticated software or advanced computer programming skills. MV has benefits as an alternative analysis, but it is more computationally intensive and seemingly impossible to perform without a computer and advanced programming skills (iteration, curve fitting, statistical F-tests proving the merit of additional Gaussian, and automation). To the credit of the authors, both Patlack and Guilford, there exists a GUI based program that allows a user to perform MV analysis. However, the program runs on Windows only, is not open source, is not actively maintained, and not obtainable without a connection to UVM. Limitations of MV analytically for trapping data is that each "event" population is biased by the length of an individual event and not the number of events itself. For example, if a data trace has 10 events, nine of them 4nm and 10ms long, and one being 20nm and 100ms long, the average of that "event" population will be more biased toward the value of the longer event than it would if the mean was calculated mathematically. As a result, ideally you need a lot of data (events) to produce a full distribution. Additionally, in MV there still is a more or less arbitrary threshold that is needed to separate populations if subtraction of the baseline is not used. However, the biggest drawback of MV is that the analysis does not actually identify individual events, but populations. This limits the ability to perform any post-analysis procedures on the individual event (ensemble averaging) that has become commonplace (and almost expected) from a modern trapping paper. Nonetheless, this method is still viable even today in the

modern trapping world as our lab as had recent success using MV with a 2020 paper detailing how a non-nucleoside substrate differential affects myosin function in a laser trap (Woodward et al. 2020).

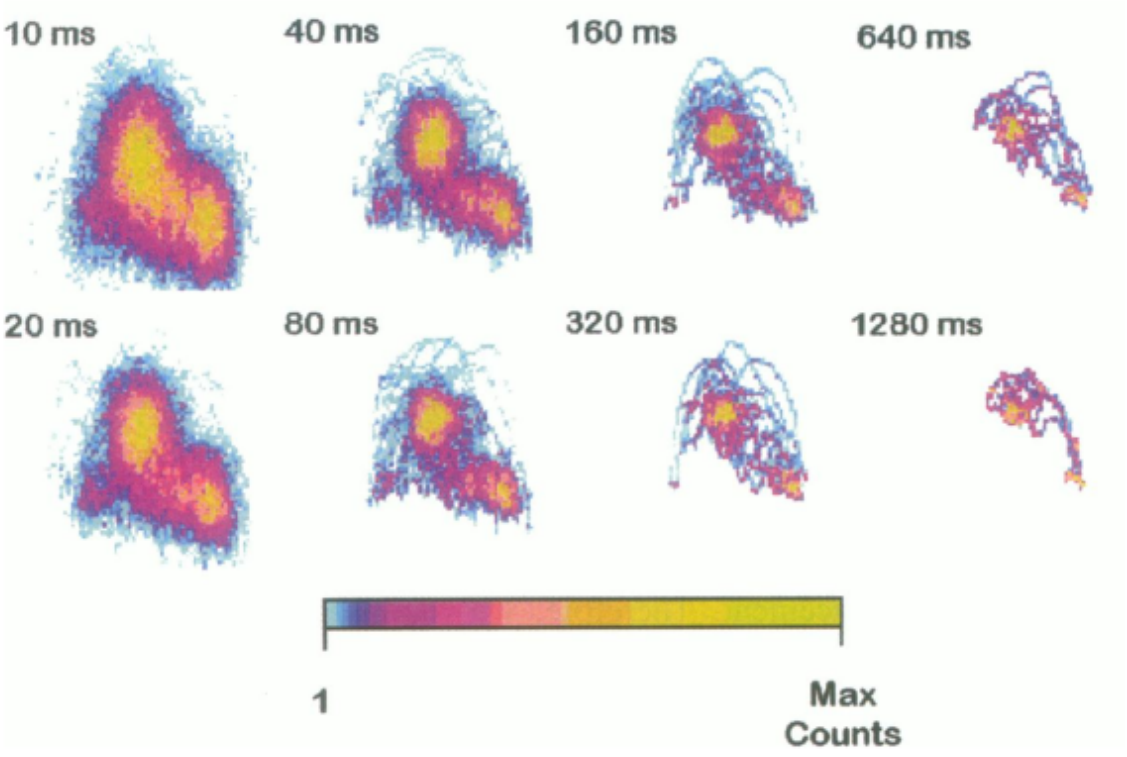

Figure 2.6. MV histograms constructed at different window width from Guilford et al. 1997

2.5.5 Page Method

For most of the 90s the previously reviewed methods, mainly thresholding and MV, was the mainstay for single molecule myosin laser trapping. Seemingly, there seemed to be large controversy over the superiority of the two methods as inferred from the review by Knight 2001. This article is a part analysis review/part introduction of the Page Method as a technique for analyzing trap data (note Veigel and Molloy are co-authors). In this review, not only is MV written-off, but the authors' (UVM crew) trapping skill seemingly outright insulted. In response to the method

Guilford et al. (1997) used to remove the baseline population to avoid arbitrarily setting a variance threshold to define an event population, Knight et al. (2001) remarks "Fig. 3c shows that the two populations can be clearly distinguished without recourse to such measures if the experimental data is of sufficiently high quality." Bold! The Page Method is an analysis that provides automatic event identification and is a re-vitalization of an older analysis technique that was originally described as a "continuous inspection scheme" by E.S. Page (PAGE 1954). In short, this method relies on using probability distribution functions (PDFs) in attempts to classify data points (of unknown origin) as a part of a certain populations, or distributions, based on comparing the probability of obtaining a data point with that specific value from a set of given PDFs in order to detect a change/switching of the underlying PDF. Knight et al. (2001) describe how to perform a version of the Page Method for the analysis of laser trapping data. First, a running mean can be subtracted from the original trapping records. The result is a removal of all displacements from the data so the "baseline" and "event" population should both be characterized as normal distributions centered around zero. However, the two populations will differ in their respective variances. The baseline will have a larger variance as dictated by Brownian motion and the event population will have a smaller variance since the increased stiffness of the myosin head dampens the effects of Brownian motion on the trapped bead's position. These variance levels can be calculated directly from the data or inferred. Since a mean and variance level can be estimated for the two populations, baseline and event, PDFs can be constructed and the probability of achieving each data point from each of the two distributions can be calculated. The log odds ratio is then expressed for each data point comparison. Due to the shapes of the two population (baseline is much wider due to higher variance) points nearest zero have a higher probability of being from the event population. This produces positive odds ratios, whereas anything with a higher probability of belonging to baseline has a neg-

ative log odds ratio. Since positive values indicate attachment events and negative values un-attachment, a zero threshold cumulative sum can be calculated over all of the resulting log odds ratios to identify the start and end of all events. Since the attachment events return positive log ratios the cumulative sum will steadily increase throughout the attachment time of a true (real) event. When the event ends negative logs odd ratio will result and the cumulative sum will return back to zero leaving a peak in the cumulative sum trace identifying the end of an event. Performing the same analysis in reverse will identify the starts of the events. There is a minimum duration threshold that needs to be set under which peaks in the cumulative sum should be ignored to reduce detection of false events. Interestingly, while this paper was submitted from a well-known trapping group and paints the Page Method in a positive light this method does not appear often or in subsequent use of analysis in their future work (it was not used in Veigel et al. (2002) - Nature Cell Biology). For what anecdotal evidence is worth, I had a lab-mate discourage me from using the Page Method as it was conveyed to me that this method was not reliably capturing shorter attachment events. Perhaps this analysis is best suited for lower ATP concentrations and/or slower motors.

2.5.6 Hidden Markov Model

In response to the controversy surrounding both the previously described analysis techniques and the inconsistency in reports of myosin's actual powerstroke size D. A. Smith et al. (2001) proposes the Variance Hidden Markov Model (HM-Model) as an alternate analysis technique that unlike the other analyses actually provides a "best-fit" to the data by removing arbitrarily set thresholds in exchange for using a kinetic model to describe the underlying probability of being in a given "state" (bound/unbound). The main goal of a HM-Model is to predict the occurrence of some un-observable event from another (related) observation. In relation the the

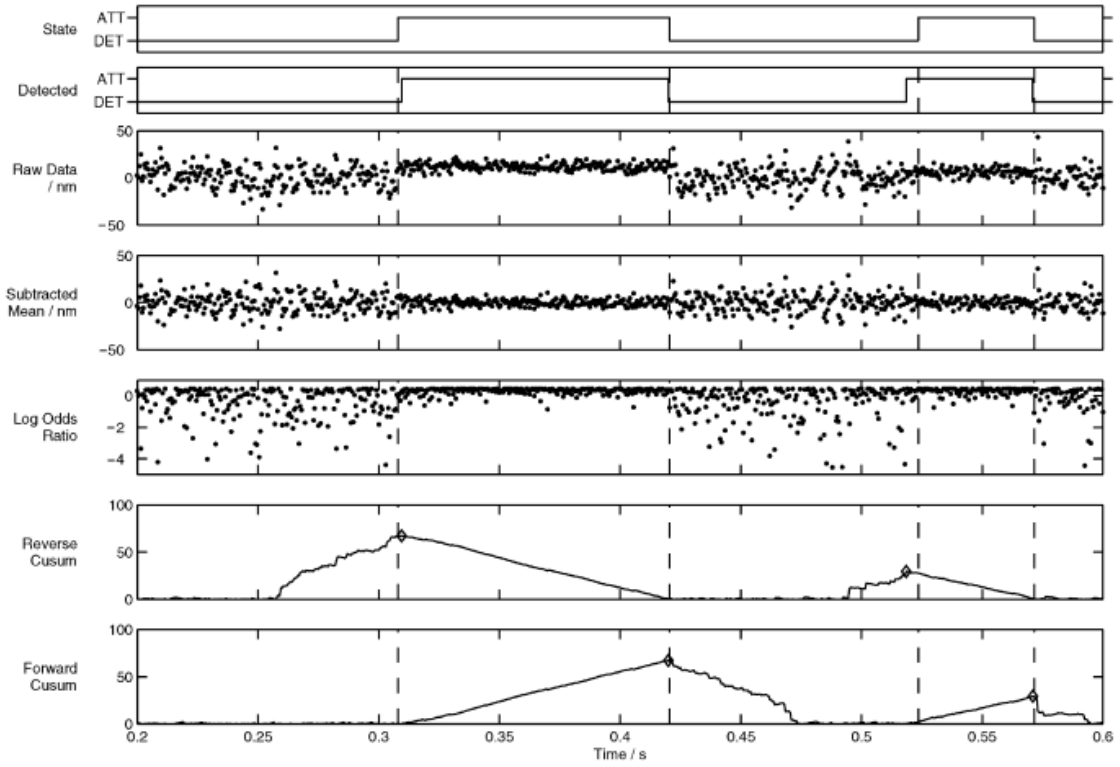

Figure 2.7. Event identification via the Page Method from Knight 2001

laser trap, the objective is to identify periods of time when myosin is bound to actin. However, you cannot actually physically see myosin bind to actin in a laser trap. This is in fact an un-observable event. But, we do know that myosin is stiffer than the laser traps, so if myosin does bind the variance of the displacement signal should decrease. This is the information in the data that is collected and that can readily be observed (bead position over time). With the HM-Model, the goal is to use the statistical characteristics of the two variance populations (unbound/bound) to predict the most probable sequence of un-observable states throughout the data. The parameters in the model include myosin's attachment and detachment rate (commonly denoted as f and g, respectively), and the variance of the unbound/bound populations. Ultimately, the probability for each variance window belonging to a certain "attachment state" can be determined by comparing the probability for each window to belong to a certain variance PDF in combination with factoring in what the previous attachment state was. In a HM-Model, a certain variance window would not necessarily be categorized as belonging to an "attachment state" just because there is a higher probability of the window to be drawn from the bound variance PDF. The HM-Model also considers the "transition probability" by taking into account the previous attachment state. The transition probability in this case is myosin's attachment/detachment rate. So, the categorization needs to determine the most likely attachment state for the current variance window based upon the conditional probability of observing a certain variance value given the prior attachment state. For an un-elegant example and if the algorithm had human thoughts perhaps it would be asking these questions to-itself while it tried to determine the attachment state given the previous state was unattached: "What's the chance of a myosin binding event occurring and then what is the chance of drawing this variance value from the attached state variance PDF?" versus "What's the chance of the myosin staying unattached and then what is the chance of observing this variance value from the unattached

variance PDF?" Though you *could* perform the attachment state de-coding by hand (it really is just multiplying probabilities and selecting the highest one to determine the state), this is performed computationally via the Viterbi algorithm. Furthermore, the parameters for the model can be estimated using the Expectation-Maximization (EM) algorithm. So a practical use case involves first estimating the model parameters with the EM-Algorithm and then using the Viterbi algorithm to perform the state sequence decoding. The HM-Model thus provides a sophisticated and robust approach to analyzing single molecule laser trap data as this technique has a simple assumption of a basic kinetic scheme for myosin dynamically binding and unbinding from an actin filament without arbitrarily defining thresholds to identify events. Furthermore, this approach was implemented when M. Capitanio et al. (2006) observed the hitch in skeletal muscle myosin II for the first time showcasing the HM-Model's ability to reliable detect true events. However, this is a more advanced approach that would require a lot more effort and knowledge (as compared to a user defined threshold) of both math and computer programming to implement and automate from scratch. Unfortunately, there are no computer programs available to easily perform this analysis on laser trap data which is probably why it is not in high spread use (even though it arguably should be).

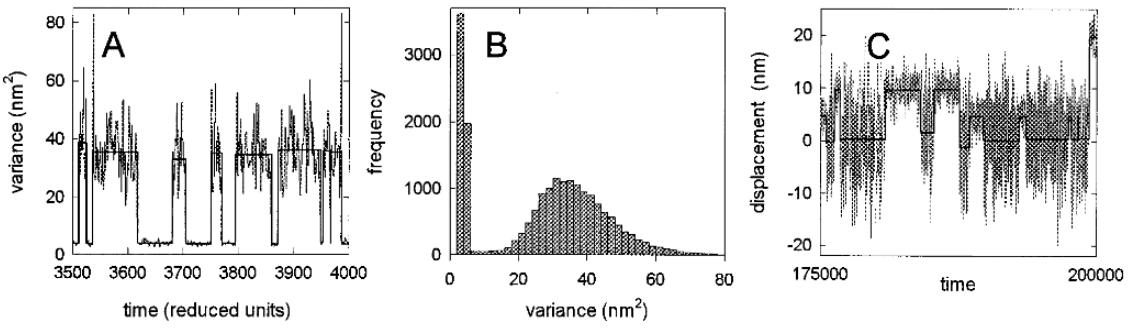

Figure 2.8. Hidden Markov Model identifies single molecule events from Smith et a. 2001

2.5.7 Ensemble Averaging

One of the advantages of using an analysis that identifies actomyosin binding events is that these methods provide information about when the event begin and ends (aka these analyses report at which data point an event start and at which data point the events end). This is quite useful information to have. For one, being informed when events are starting/ending allow the user to be able to visually inspect the data and the resulting analysis to decide whether the analysis appears to be identifying "true" events or not which allows the user to be more confident in their data if they are visually pleased with the results. But also, having an analysis program that identifies individual events allows additional post-analyses to be performed. A common such test for laser trapping data is ensemble averaging. To ensemble average trapping data first you need data that has been analyzed with some sort of event identification analysis. Once all the data has been analyzed and events identified there is a couple unusual transformations that occur. Furthermore, a complete ensemble average consists of both a forward and backwards ensemble average which differ by the initial alignment of the events. Forwards ensemble averages are aligned at the start of the events and the backwards ensembles are aligned at the end. To conduct an ensemble average, first all events are subset out of the original data trace and are extended to the length of the longest event. Then the events can be aligned horizontally by being placed on the same relative time scale and each point averaged vertically so the first data point of the first event is averaged with the first data point of the "nth" event. The results of the ensemble average is "one event" that represents the average response of all the events. By performing this analysis additional information can be estimated from trapping data. For instance, with the forward ensemble averages the rate of the first and second powerstroke can be estimated; however, providing estimates for the rate of the first powerstroke is rare as the rate of the first powerstroke is far greater than the time resolution of a standard rate. Some

researchers ignore this rate, but this rate can still be fit and used to represent the rate at which the unbound to bound transition occurred for a given condition with the caveat being the rate is not reflective of the rate of the actual powerstroke, but one that would reflect the powerstroke and the resulting movement of beads through solution. Ensemble averaging has been used extensively to measure both the size and rate of the second powerstroke, sometimes called "the hitch." Additionally, since the hitch is often associated with the release of ADP many use the rate of the second powerstroke as a surrogate measure of the ADP release rate that can be estimated from trapping data. The size of the hitch can be estimated from a floating parameter to the exponential fit that estimates the rate, or by subtracting the beginning position of the backwards ensemble from the final displacement from the forward ensemble. Lastly, the second order binding constant of ATP to myosin can be estimated from an exponential fit to the backwards ensemble. As a result, ensemble averaging serves as a powerful post-analysis tool which can provide important kinetic and mechanical insights to the originally collected data set.

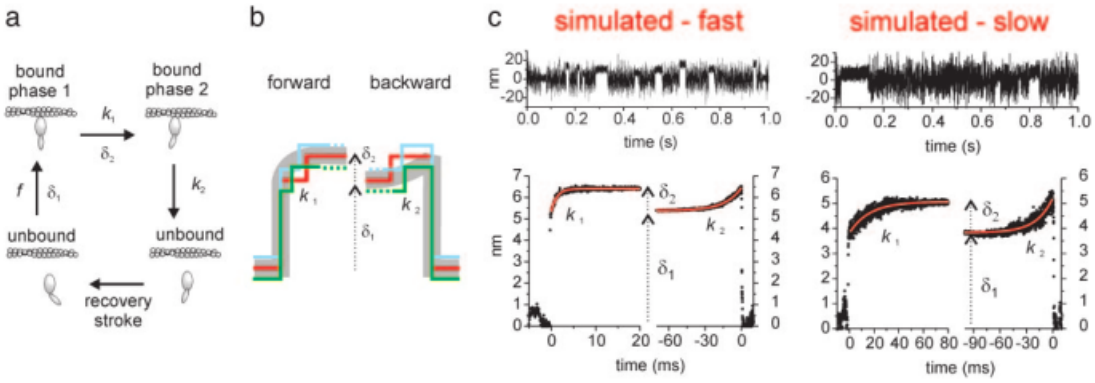

Figure 2.9. Ensemble averaging data from Capitanio 2006.

2.6 Ultra-fast force clamp (UFFC)

In almost all of the previously described analyses techniques in Chapter 2.6 the variance of the trapping signal is used to somehow differentiate between myosin being either attached or un-attached from actin. While this is a reliable method in regards to detecting single molecule events, the time resolution afforded by the standard laser trap setup of two beads stuck in stationary traps is limited in which these analysis method can be used. As a result the use of the signal variance for event detection can only be pushed so far. In a standard laser trap setup, the time resolution is ultimately limited when using a variance driven analysis method due to the roll-off frequency of the baseline signal of the trap, dictated by brownian motion and the stiffness of the traps:

$f_c = (1/2\pi) * (kx/6\pi\eta r)$

Unfortunately, the limited time resolution is not a simple issue related to the analysis technique used or even to the sampling frequency. The problem with the limited time resolution in a standard laser trap setup using an event identification program (or when applying real-time feedback) based on changes in system stiffness/variance is that there is a lack of signal in the necessary frequency range (Knight et al. 2001). This means that changes in variance are only detectable for frequencies far less than the corner frequency of the trapping signal (Marco Capitanio et al. 2012) leaving the shortest detectable events to be ~5-15ms in a typical trapping setup (Knight et al. 2001; Marco Capitanio et al. 2012) as temporal resolution is inversely proportional to the roll-off frequency (Neuman and Nagy 2008) and most research groups report roll-offs between 300-500 Hz (Veigel et al. 1998; Guilford et al. 1997). In theory, the temporal resolution can be increased under standard trapping conditions by increasing system stiffness or by decreasing the drag on the beads (Neuman and Nagy 2008). But in practice, increasing baseline stiffness would then decrease the signal-to-noise ratio that is typically used to detect binding in three-bead assay. To combat the lim-

ited temporal resolution in the standard laser trap setup people started "wiggling" one of the traps. Veigel et al. (2003) was the first to "wiggle" on of their traps in a myosin based three-bead assay. The motivation of the paper was to apply load directly to a single myosin motor in order to probe the underlying mechanisms of the "Fenn Effect." Here, the authors applied a 1kHz oscillation (sine wave) to one of the traps (high frequency, low amplitude). Attachment events were then able to be identified as deviation from the assigned amplitude to the oscillating trap. This effectively decreased their time resolution to ~1ms. Marco Capitanio et al. (2012) took this approach to another level with the introduction of the Ultra-fast force clamp (UFFC). While Veigel et al. (2003) had the time resolution to asses the load dependence of the ADP-bound state in smooth muscle myosin II at low ATP concentration, 1-ms time resolution was still too slow to directly observe or test the load dependence of the powerstroke itself. In standard optical trapping setup the "powerstroke" is not seen and the transition between unbound/bound appears instantaneous. In fact, even in the ensemble averaged data of standard optical trapping data, the "rate of the first powerstroke" is often ignored because the powerstroke rate occurs faster than the time resolution of the trap and the unbound-to-bound transition is influenced by the terminal velocity of a damped bead moving through solution. Additionally, smooth muscle myosin has a two-fold slower ATPase rate (Harris and Warshaw 1993) than skeletal muscle myosin II. Which brings up the major problem when trying to study skeletal muscle myosin II - *it is fast*. Moreover, skeletal muscle myosin II has a low duty ratio and is non-processive. This means that it spends the majority of its time off-actin and only transiently interacts with an actin filament in a stochastic manner which means it only spends a few milliseconds on actin at saturating ATP concentrations.

The UFFC has micro-second temporal resolution and sub-nanometer spatial resolution. To reiterate, the UFFC has MICRO-SECOND temporal resolution and SUB-

NANOMETER spatial resolution. If you don't think this is cool *you should probably stop reading this dissertation now.* With UFFC not only can single powerstrokes be observed, but load can be applied to the actual powerstroke as well. The increased time resolution is applied with a similar principle to what Veigel et al. (2003) performed - "wiggle" the traps. The following sentence might be the biggest understatement/oversimplification in this entire dissertation. In UFFC, both traps are "wiggled" simultaneously, very quickly. The basic setup is still a three-bead assay, but once a dumbbell setup is formed, both traps are rapidly displaced back and forth which results in a triangular wave being imposed on the setup. The side-to-side displacements are performed by first putting equal and opposite forces on both of the beads (via AOD control), and then additional force is added to one of the traps which steers the setup in a certain direction at a specified force level. Once, a pre-configured distance is reached (~200nm), the additional load is then revoked from the one trap and added to the other in order to switch the direction of the setup. Switching directions of the movement allows the actin filament to remain within binding distance to the myosin on the mogul. One advantage of UFFC is that the dumbbell setup is always experiencing the load, so when a myosin does bind, the load will be instantaneously (well, near-instantaneous…this time depends on the the stiffness) applied to the myosin as there is no waiting period for a feedback system to engage once an actomyosin interaction is detected. Events are detected by converting the raw positional data (bead displacement over time) into a velocity measure and applying a threshold. The velocity of the dumbbell ends up being equivalent to the total force applied to the system divided by the viscous drag of the dumbbell setup $v = F_{total}/drag$. Since the UFFC is designed to apply a constant force, when myosin binds the traps will rapidly stop moving in order to maintain the desired force level. This results in the velocity transformation of the raw UFFC displacement record forming a double Gaussian with the bound population being centered on zero (nm/ms). Currently, only two UFFC

experiments have been performed with myosin. The original UFFC experiment was performed with skeletal muscle myosin II Woody et al. (2019). Woody et al. (2019) performed UFFC with cardiac myosin II under both 0mM and 10mM-P_i. As previously described, the UFFC provides the perfect test of the main proposed question of this dissertation - "What is the relative timing between the powerstroke and P_i-release?" because UFFC allows for direct observation of the powerstroke and this can be tested under both 0mM and 30mM-P_i concentrations. This technique allows to test the question without a mutation that slows myosin's kinetics (i.e. "making a slower mouse") because it has the necessary time resolution to directly observe if the presence of high P_i levels, which increase the probability of myosin re-binding to the active site, can prevent and/or delay the powerstroke (i.e. UFFC is the "better mouse trap"). Indeed, Woody et al. (2019) observed that the presence of 10mM P_i did not alter the rate of the powerstroke in cardiac myosin. Thus concluding that the powerstroke precedes the release of P_i from the active site; however, structural biologists have disputed these claims as mis-interpretation of the results of their UFFC data and actually see Woody et al. (2019) as provided evidence that P_i-release gates the powerstroke (Robert-Paganin et al. (2020)). Clearly, there is still a need to perform UFFC with high P_i, especially with skeletal muscle myosin II since it has yet to be done.

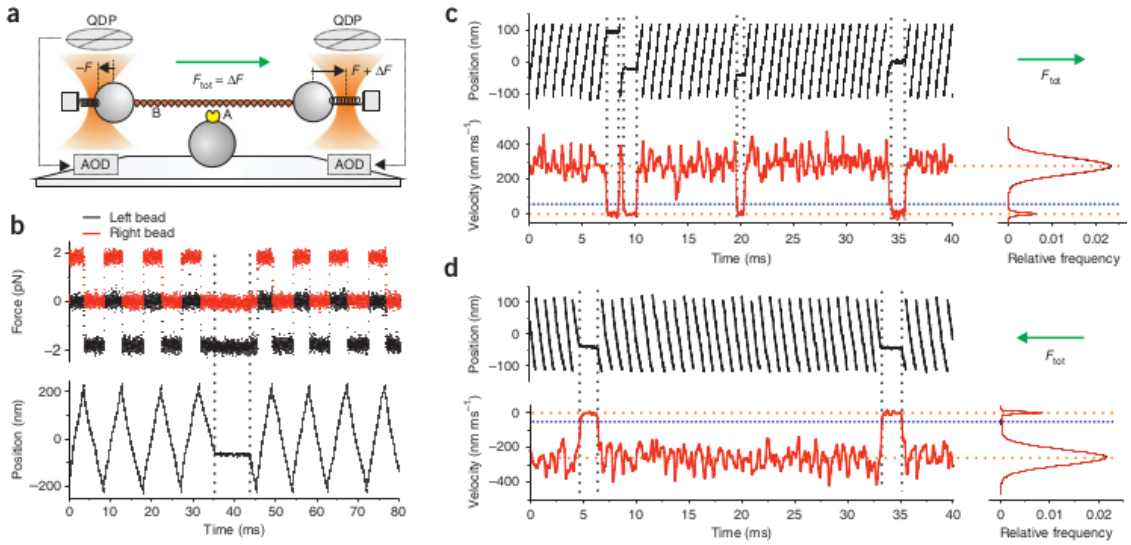

Figure 2.10. The Ultra-Fast Force Clamp

CHAPTER 3

METHODS

3.1 Protein Isolation and Expression

3.1.1 Myosin V expression

Myosin V S1 is expressed (baculovirus system) with the first 792 amino acid residues which includes 1 IQ domain as detailed previously by the Yengo Lab (Gunther et al. 2020). Additionally, expressed myosin V contains the N-terminal tetracysteine motif, C-terminal Myc, and C-terminal FLAG tags (Trivedi et al. 2013, 2015, 2020; Gunther et al. 2019). The S217A mutation was introduced (serine to alanine) using QuikChange site-directed mutagenesis (Stratagene), co-expressed with calmodulin, and purified with FLAG affinity chromatography.

3.1.2 Skeletal muscle myosin II isolation

Fast skeletal muscle myosin II was isolated from chicken pectoralis muscle (Diemand Farm, Wendell, MA). All procedures during isolation were carried out in a cold room or performed on ice. Isolation was performed as previously described by the Debold lab (Woodward et al. 2020; Unger and Debold 2019; Longyear, Walcott, and Debold 2017) by Mike with a protocol similar to those of Margossian and Lowey (1982) with minor modifications. In short, chicken breast muscle is passed through a meat grinder and rinsed with 0.2M EDTA. 2 mL of Buffer A (Extraction buffer consisting of 0.3M KCl, 0.15M KPi, 20mM EDTA, 5mM $MgCl_2$, 3.3mM ATP, and 5mM DTT at pH 6.7) is added per gram of tissue including 5mL of protease inhibitors. This is mixed for 12 minutes with an overhead stirrer. The reaction is stopped with

a 4X dilution into water which is then mixed and filtered. After precipitate settles it is centrifuged at 10,800g for 10 minutes at 4C and the resulting pellet is resuspended with Buffer B (Suspension buffer consisting of 1M KCl, 60mM KPi, 20mM EDTA, and 5mM DTT at pH 6.7) and mixed gently before being left to dialyze overnight. Actomyosin is then precipitated and centrifuged at 41,171g for 1 hour at 4C and the resulting supernatant is diluted 10X with water. Clear supernatant is siphoned off and the rest is centrifuged again at 10,800g for 15 minutes at 4C. Supernatant is poured off and precipitate is resuspended with Buffer D (Resupsension buffer consisting of 3M KCl, 50mM KPi, and 5mM DTT at pH 6.7) before being dialized overnight for a second time against Buffer E (Dialysis buffer consisting of 0.6M KCl, 50mM KPi, 1mM NaN_3, and 5mM DTT at pH 7.0). After the dialysis, myosin is clarified with an ultracentrifugation at for 2 hours at 4C, concentration determined, snap frozen with liquid nitrogen, and stored at -80C.

3.1.3 Actin isolation and labeling

Acetone powder was prepped from the remainder from the myosin isolation (with the leftovers from the filtered cheesecloth) and actin purification was performed from the resulting acetone powder as described by Pardee and Spudich (1982) with modifications. Briefly, acetone powder was finely ground and mixed with extraction buffer (2mM Tris Base, 0.2mM $CaCl_2$, and 0.005% NaN_3 at pH 8.0) and stirred with an effort to minimize creation of bubbles. The resulting solution is spun at 28960g for 20 minutes and supernatant filtered off and kept aside. Additional extraction buffer added to gel-like precipitate and centrifuged a second time with the same specs with the supernatant filtered off and combined with the previous. Actin is polymerized from the resulting supernatant by addition a final polymerization solution (50mM KCl, 2mM $MgCl_2$, and 1mM ATP). Salt is added to slowly to prevent "salt shocking" the proteins before being left to stir overnight. The next day, a high salt wash

(increase KCl to 600mM) removes tropomyosin from the f-actin and then then the sedimentation of f-actin performed by centrifuging at 205835g for 60 minutes. The precipitate is transferred to a homogenizer and resuspended with extraction buffer. A 4 day dialysis is performed with extraction buffer additionally containing ATP and DTT to de-polymerize actin. After dialysis the resulting G-actin is clarified with an ultracentrifugation at 200,000g for 60 minutes. After actin is polymerized by adding 10mM Imidazole (pH 7.0) and 1mM $MgCl_2$ and dialyzed against final storage buffer (4mM Imidazole, 25mM KCl, 2mM $MgCl_2$, 1mM NaN_3, and 0.01mM ATP at pH 7.0). After calculation of final concentration actin is snap frozen in liquid nitrogen and stored at -80C. After isolation actin can then be labeled with 100% TRITC for use in vitro motility or mixed with a 50:50 TRITC/Biotin solution for use in the three-bead laser trap assay.

3.2 Laser trap assay

The laser trap assay was performed as previously described by the Debold Lab (Woodward et al. 2020; Unger and Debold 2019; Longyear, Walcott, and Debold 2017) with special considerations for the expressed myosin V. Single molecules of myosin were adhered to a nitrocellulose coated microscope slide containing 3µM glass pedestal beads with an additional coverslip glued on top for construction of a "flow-cell." The final myosin concentration of ~0.8-1µg/mL was added after to introduction of anti-myC antibody (0.8µg/mL, Sigma Inc.) which provided a binding interface for the expressed myosin on the surface. Bovine Serum Albumin (BSA) was used to block the remainder of the surface before the addition of final buffer. The final buffer consisted of an actin buffer (91mM KCl, 1mM EGTA, 4mM $MgCl_2$, and 1mM DTT at pH 7.0) mixed with 100µM ATP, and an oxygen scavenger system (29mM glucose, 1.5mM glucose oxidase, and 80 units catalase) at pH 7.0. For 30mM P_i experiments KCl was reduced in order to maintain the 125mM total ionic strength to match the

control 0mM P_i experiments. The concentration of TRITC/Biotin labelled actin filaments and neutravadin/streptavidin coated 1 micron beads (Bangs Lab Inc) was varied at trappers discretion. Bead-actin-bead "dumbbell" setups were constructed using a three axis piezo controlled state (Mad City Labs) with a time shared laser trap between two positions. Experiments were performed at 1.5 Watts laser power and actin filaments pretension to 3-4pN. The resulting system stiffness of the two laser traps and the pretension across the filaments was 0.04pN/nm, determined via the equipartition method (DUPUIS et al. 1997). Bead position was tracked using a four quadrant photodiode with a sampling rate of 5kHz.

3.3 Ultra-fast force clamp

The UFFC data was collected under the same experimental conditions and buffers as described in the section 3.2 for the standard laser trap assay, but full length fast skeletal muscle myosin IIx was adhered to the nitrocellulose coated coverslips instead of the myosin V and anti-body combination. Since UFFC is an extension of the standard three-bead assay implementation was similar in regards to setting up a dumbbell. However, in order to increase the speed that the dumbbell was able to move through solution when the force clamp was engaged smaller 510nm beads (Bangs Lab) were coated with neutravidin (31000, Pierce) for use in the UFFC. Decreasing the radius of the beads reduces the Stoke's drag coefficient since $\beta = 6\pi\eta r$, where β represents the drag coefficient, η the viscosity of solution, and r is the radius of the bead. Furthermore, the drag coefficient is inversely proportional to the velocity of the dumbbell setup as given by $velocity = F_{total}/\beta$. The smaller the drag the faster the dumbbell can move. Consequently, the increased velocity of the dumbbell setup in the un-attached state increases the time resolution and signal-to-noise ratio of the resulting data. Force was pre-determined for each experimental condition and set by calculating the bead's displacement from the center of the trap and converted to a

force since $F = -kx$, where x is the bead's displacement and k is the stiffness of the trap. The trap stiffness was similar to the standard laser trap experiments at roughly 0.04 pN/nm calculated by analysis of the power spectrum. Positions of the traps were controlled through the AODs and a custom LabView program. Bead position was collected at 200kHz sampling frequency. The total feedback delay was around 8;micro:s, this is the total time it takes for the computers to detect changes in the beads position relative to the center of the trap, communicate the information, and for the AODs to respond to the changes.

Actomyosin interactions in UFFC are identified by applying a threshold the velocity transformation of the raw displacement data that is generated during data collection. The velocity was calculated instantaneously on a point-to-point basis and the results smooth with a Gaussian filter. The velocity transformation results in a double Gaussian distribution with two peaks corresponding to the average velocity of the bound and unbound populations. The bound population velocity is centered around zero because as myosin binds actin and imposes its own stiffness/drag the UFFC will feedback in attempts to apply a consistent force to the dumbbell causing the traps to stop moving. The threshold is set at the point along the joint PDF of the double Gaussian where the probability of crossing the threshold due to noise from the unbound or bound event is equivalent. The threshold was then optimized for each record to decrease the number of false events detected to <1%. If false events exceeded 1%, the SD of the Gaussian filter was increased to further smooth out the data in order to decrease the probability of a baseline noise artifact crossing the threshold. Note that usually smaller SD of the gaussian filters could be applied at great forces due to an increase in force subsequently increasing the signal-to-noise ratio since the baseline velocity is faster to achieve higher forces. Additionally, there is a correction factor that is applied to determine the start and end of the events that is a result of the optimal threshold being closer to the peak of the bound population in the

velocity distribution that is a result of the bound population having a narrower peak (smaller SD) since myosin stiffness is greater than the trap stiffness. After event identification, events were ensembled averaged as by synchronizing events in the x and y dimensions by applying linear regressions to the baseline prior to the start of the event (when the bead is moving at constant velocity) and overlaying events at the point where the linear regression intersected the start of the event as ID'd prior in analysis. The resulting ensembles could be fit with a model consisting of a linear portion that described the delay before the powerstroke and a double exponential reflecting the kinetics/mechanics of myosin going through the first and second powerstroke. Ensemble averages are typically calculated separately for the three populations of event durations that are prevelant in UFFC experiments (short, intermediate, and long) since these events represent different mechanochemical schemes of an actomyosin interaction.

3.4 Step-by-step single molecule event identification

This is a "step-by-step" walk through of the Hidden-Markov/Changepoint Analysis we use to analyze our single molecule laser trap data and includes everything on the journey from raw data to analyzed trace and everything on the way…buckle up. This section is a lot cooler if you are reading online and includes the R code to reproduce this by hand. You can download the data here

3.4.1 Raw data

Here is a raw data trace. This is unprocessed data as-is from the trap computer. The data is relative position of the bead in mV over time:

The data record is 89.1576 seconds long and has an average position of 6.2968527 mV.

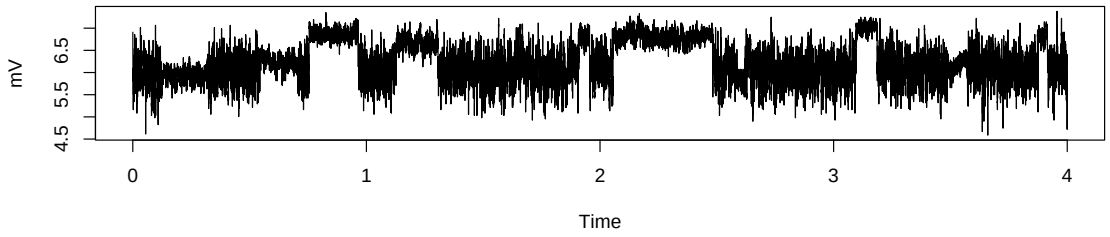

Figure 3.1. Raw trap data.

3.4.2 Processed Data

The first step of the analysis is removing the "baseline" by centering the mean around 0. This can either be done by simply subtracting the baseline mean from every data point or by performing a piecewise linear detrend on the whole record. The latter accomplishes two things: **1)** Centers mean around 0 and **2)** removes any drift (i.e. wander correction). Additionally, in the **lasertrapr** app you can find the average baseline position by using a mean variance transformation of the data to select the baseline population or by selecting a quiescent period of the data where no binding events occur to calculate mean baseline position. Here we will detrend the data and convert from mV to nm using a "Step Calibration." The step calibration is performed by moving the microscope stage a known distance, say 200 nanometers, and measuring the resulting change in the mV signal. We then can estimate the number of nanometers per mV.

The mV-to-nm conversion calibrated around the time this data trace collecting we are analyzing know was 30 nm/mV. We can convert our raw data from mV to nm and detrend the data (or visa versa).

3.4.3 Running Mean & Variance

Running Mean & Variance

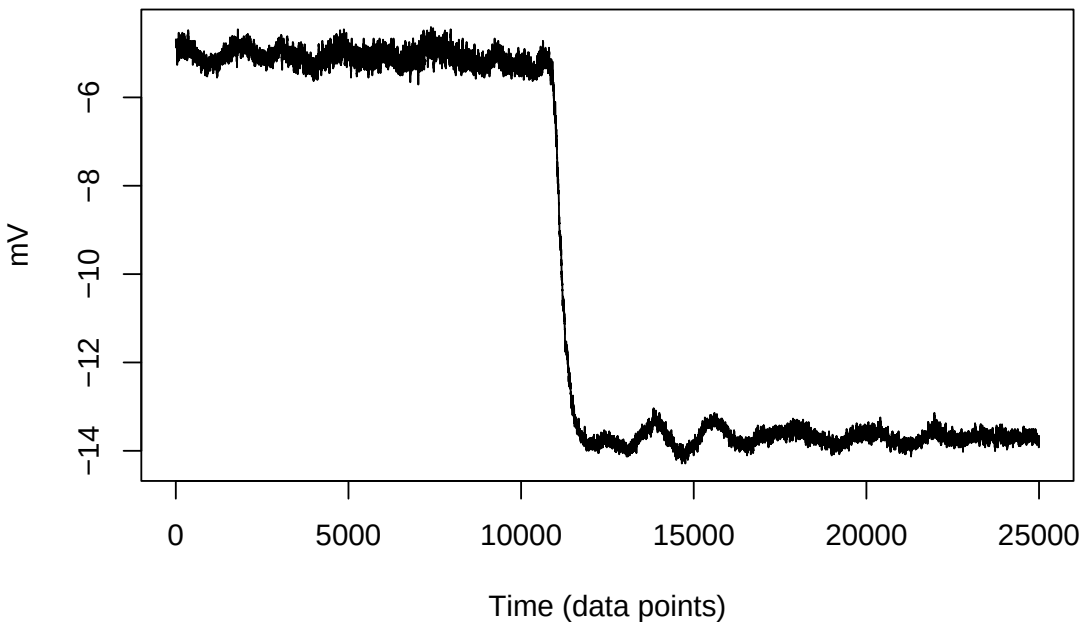

Figure 3.2. Example of a step calibration. Stage was moved 200nm

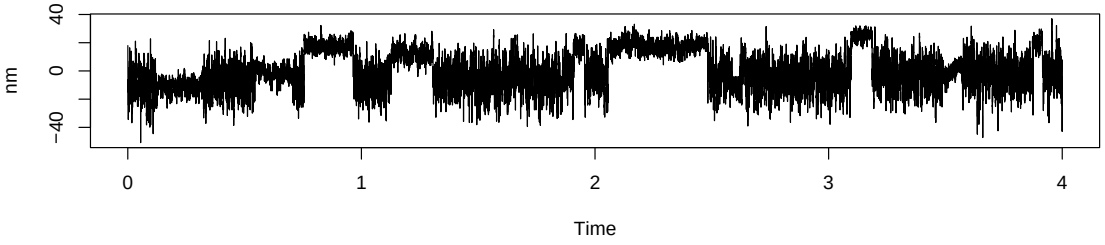

Figure 3.3. Example of processed trap data

The next step is to transform the data for the HM-Model by calculating both the running mean and variance of the data trace. This analysis uses a 150 datapoint window that advances by sliding 75 data points each time (half the window width). This is done to decrease the correlation between neighboring windows:

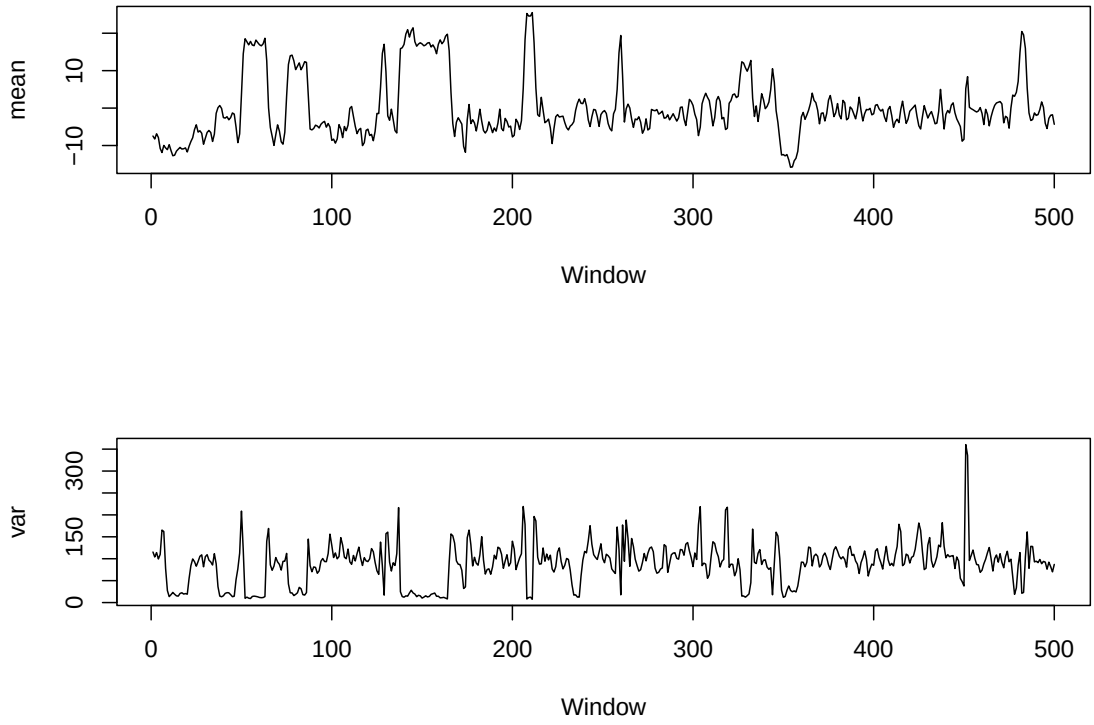

Additionally, we can plot these datasets against each other to see the mean vs. variance for each window:

3.4.4 Hidden-Markov Model

The data is now ready to have events identified with a Hidden-Markov Model. We first need to initialize the model with guesses of the initial state probabilities and the transition probabilities for our 2-state model. State 1 is when myosin is unattached from actin and state 2 is attached. We need to guess 6 different numbers.

1) Probability of initially starting in state 1
2) Probability of initially starting in state 2

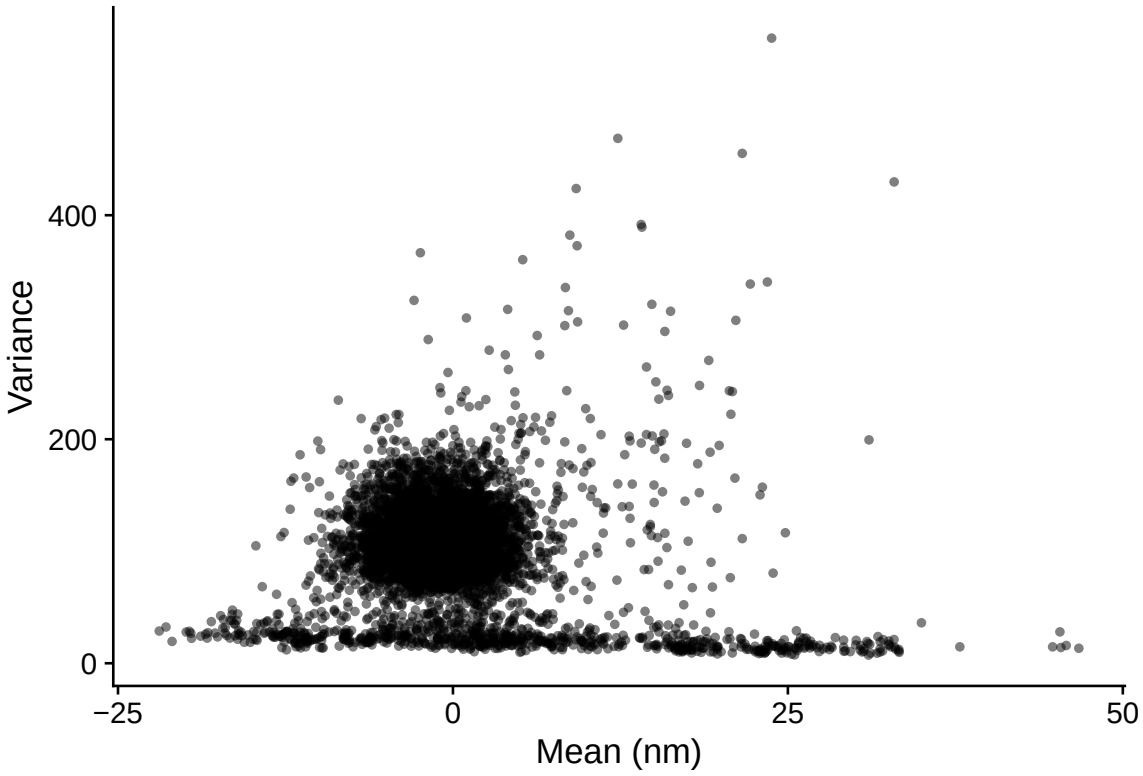

Figure 3.4. Mean/Variance Plot

3) Transition probability from going from state 1 to state 1

4) Transition probability from going from state 1 to state 2

5) Transition probability from going from state 2 to state 1

6) Transition probability from going from state 2 to state 2

I prep the data so it usually always start with baseline (i.e. state 1) or will trim it so the trace does though 99.9% this just occurs so we will give guess that 98% probability of starting in State 1. Probability of starting in state 2 is then 1 - [Prob. S2] = -.02. I then assume that these are both stable states and that there is a high probability of tranisitioning from state 1 to state 1 or state 2 to state 2. By the same logic above the transition probabilites are guess and our 6 probabilities above are:

```
## [1] 0.98 0.02 0.98 0.02 0.02 0.98
```

We will also have to make guesses of the statistical characteristics of the 4 underlying Gaussian distributions (2 states for each the running mean and running variance). To do this we will estimate the mean and standard deviation of each of the Gaussian. The 8 numbers that follow are:

1) Guess for the mean of the variance for State 1. -calculated by taking the mean of the running variance

2) Guess for the sd of variance for State 1 -calculated by the taking the sd of the running variance

3) Guess for the mean of mean for State 1 -hard coding to 0 because we centered baseline around 0 when we processed the data.

4) Guess for the sd of mean for State 1 -calculated by taking the sd of running mean

5) Guess for the mean of variance for State 2 -estimated as half the value as state 1 (signal-to-noise 2:1)

6) Guess for the sd of variance for State 2 -#2/2 because of stiffer system when myosin attached

7) Guess for the mean of mean for State 2 -hard coded at 5nm (estimated size of the powerstroke)

8) Guess for the sd of mean for State 2 -coded as twice #4 since there will be positive and negative displacements

```
## [1] 101.69  45.56   0.00   6.47  50.85  22.78   5.00   6.47
```

Once we estimate the starting point the model can be fit. The HM-Model will optimize all the parameters we just defined using the Expectation-Maximization (EM) Algorithm. The resulting model summary (Re1. = "Response 1" and is the variance signal while Re2. = "Response 2" and is the mean signal):

```
## converged at iteration 12 with logLik: -47137.21

## Initial state probabilities model
## pr1 pr2
##   1   0
##
## Transition matrix
##         toS1  toS2
## fromS1 0.974 0.026
## fromS2 0.180 0.820
##
## Response parameters
```

```
## Resp 1 : gaussian
## Resp 2 : gaussian
##     Re1.(Intercept) Re1.sd Re2.(Intercept) Re2.sd
## St1         113.302 36.224          -0.758  3.950
## St2          22.375  8.612           5.185 13.816
```

Starting from the first line in the summary we can see that the model gives a 100% probability that this record starts in baseline (state 1). The transition matrix is straightforward to read and these probabilities could also be used as estimates of on/off rates although currently we have not been using these. Lastly, the "response parameters" are the optimized characteristics of the Gaussian distributions describing each of the state 1 and state 2 normal distribution for both the mean and variance signal. The results are that the variance distribution for state 1 has a mean of 113 (SD of 36) and state 2 has a variance of 22 (SD of 8). This gives a signal to noise of a little more than 5:1 in the variance signal. Furthermore, the baseline mean has a mean of -0.7 (SD of 4) and state 2 mean is 5.1 (SD of 13).

Now knowing these parameters we can extract the most probable state sequence through the trace via the Viterbi Alogorithm. Here is a table of the posterior states (columns are state = viterbi state, S1 & S2 are the delta probabilities of being in each state):

state	S1	S2
1	1	0
1	1	0
1	1	0
1	1	0
1	1	0
1	1	0

We can now construct another Mean/Variance plot using the running window transformation and this time color code the windows by State:

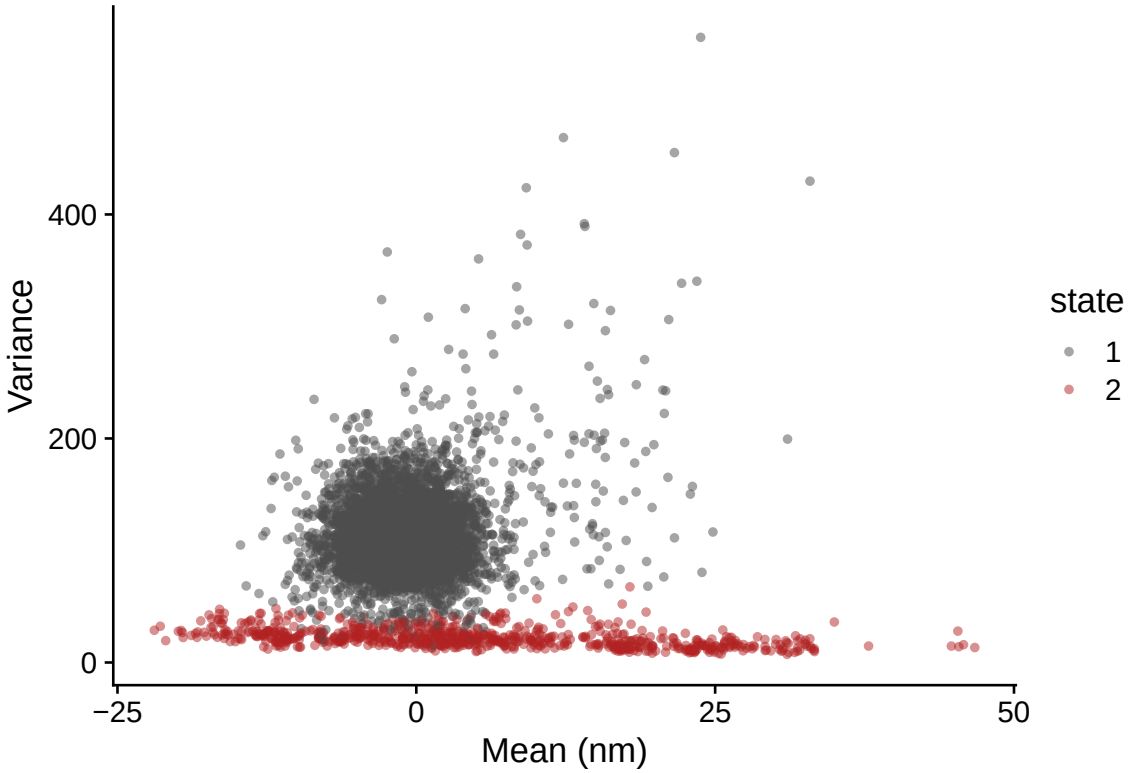

Figure 3.5. Mean/Variance Plot colored by State

At this point I think we have completed the hardest part of laser trap analysis - **picking events**. Now we need to find the the peak displacements (and subsequently forces), time off, and time ons for each event. I call this 'measuring events' (because in reality I feel like these could be simple measurements you could make with a ruler).

3.4.5 Measure Events

The HM-Model state sequence decoding assigns every running window a 1 or a 2 describing the state that the window most likely belongs to. So all we are given is a long list of a 1-2 indicator that is the same length as our running mean/variances.

We need to calculate the number of 1's and 2's that occur in a row and then calculate the cumulative sum of these 'in-a-row' counts to get the indices of when the events start/stop in running window time. Here is the number of 1's and 2's that occur in a row.

lengths	values
8	1
12	2
16	1
10	2
5	1
12	2

The table can be read that the raw trace starts with 8 windows of state 1 baseline noise followed by 12 windows of a state 2 event etc.

On times in milliseconds can be estimated by taking those state 2 'in-a-row' lengths and converting them to 5kHz time and then to ms. The conversion from window time to 5kHz can be calculated by the dividing the length of the raw/processed data by the length of the resulting running mean/var calculations:

```
## The conversion between raw data and running windows is  75
```

This also works out to be the advancing window sliding distance in the running mean/var calculations. Estimating on-times is then straightforward. Multiply state 2 'in-a-row' length by the conversion and then divide by sampling frequency (5000) to get into seconds and multiplied by 1000 for ms.

The same idea can be applied to the state 1 baseline to get the off times. In the process the first and last off-times are excluded because in reality we do not know when the last event before our first recorded event actually occurred. Additionally, the last baseline/state 1 ends because we stop recording so that is also not a true measure. Here is the table of on/off times:

n_event	hmm_state	num_windows	length_5kHz	time_on_ms	time_off_ms
1	2	12	900.27869	180.05574	NA
2	2	10	750.23225	150.04645	240.07432
3	2	12	900.27869	180.05574	75.02322
4	2	11	825.25547	165.05109	180.05574
5	2	1	75.02322	15.00464	630.19509
6	2	27	2025.62706	405.12541	120.03716

In this table the *time_off_ms* column refers to the off time that occurred prior to the event.

Moving along and to make this information more helpful in being able to really ID where the events are stopping and starting we can take the cumulative sum of these 'in-a-row' lengths that will give us the running window indices of the start/stop of the events. This will help us chunk out the events to measure step sizes. After calculating the cumulative sum of the 'in-a-row' lengths we can make a new table with 2 columns. One column *state_1_end* indicating the window which is the last window in a series of baseline and a *state_2_end* column that is the last window of an event series.

state_1_end	state_2_end
8	20
36	46
51	63
75	86
128	129
137	164

The result is the running window indices of the window before the event starts and the window that ends the event. By adding one (+1) to the *state_1_end* value we get the index of the start of each event.

```
## So the first event is between indices 9 and 20
```

We can estimate the step size from the running windowed data. To get the step size we find the position of the running window with the greatest absolute value and take its real value. Finding the index of the window with the greatest absolute value let's us also find the peak of negative events more accurately than just taking the max right off the bat.

Now this would give us step size estimates since we already processed the data to be centered around 0. However, our baseline signal does not always return to 0 after an event. To get a more precise estimate of our step sizes by the same logic we can calculate the average of the baseline noise prior to each event and then subtract the step size estimate from the baseline prior to the event.

This results in a table giving the mean of the baseline before each event (avg_s1), the estimated step size (avg_s2), and the differences between the 2 (diff) representing the final step size the program reports for each event.

avg_s1	avg_s2	diff
-9.2145628	-12.734709	-3.520146
-6.9028608	-3.127884	3.774977
-0.6201406	18.654526	19.274667
-4.1346721	14.146184	18.280856
-4.5201374	17.046019	21.566157
-0.9125085	21.452987	22.365496

3.4.6 Direction Correction

Admittedly, sometimes the actin filament is oriented in the wrong direction. To compensate for backwards filaments the program has a so-called 'direction-correction' and will auto-magically flip the raw trace if the filament was oriented the wrong way. What happens here is after analyzing step sizes if the program identified more negative events than positive events it assumes backward-filament orientation in the trap and

flips the trace horizontally over the x-axis by multiplying every value by negative one (-1). Now if the records were flipped so were the calculated step sizes and these new values reported along with the force measures that are calculated by the step size multiplied by the user-inputted nm -> pN conversion. These values are added to the on/off time table previously calculated.

3.4.7 Changepoint Analysis

Since we identified the events we can also perform ensemble averaging with a little more work. Unfortuntely, preparing the data for the HM-Model by transforming into running mean/variances decreased our time resoultion as we lost a lot of information. Our original number of data points collected is 445788, whereas the number of data points (windows) in the running mean/var is 5942.

The resulting start/end of each events are really just estimates. To get better start of event estimates the program uses changepoint analysis on the transition periods into and out of each event to better estiamte the start of each event in the original sampling frequency.

To obtain the transition periods from raw data in 5kHz time the running window indices from the state_1_ends and state_2_ends are converted to 5kHz time by the conversion ration of ~75 we previously calculated as the ratio between the number of datapoints in the raw data to the data points in the running mean/var calculations.

More specifically, the program finds the running window index of ~1.5 windows back into the baseline from the *state_1_end* window and the index of the to the first state 2 window and converts back into 5kHz time to supply a slightly larger transition window to analyze for the 'true' event start. Doing this for every event we obtain a new table with 5kHz time indices that *should* contain the transition into every event:

The changepoint analysis is actually performed on a new running variance of the processed data with a variable length window width. Here I use 5 datapoints

(1ms) because the trace has exceptional singal-to-noise. This running transformation advances one point at a time. The resulting running variance transform looks like this:

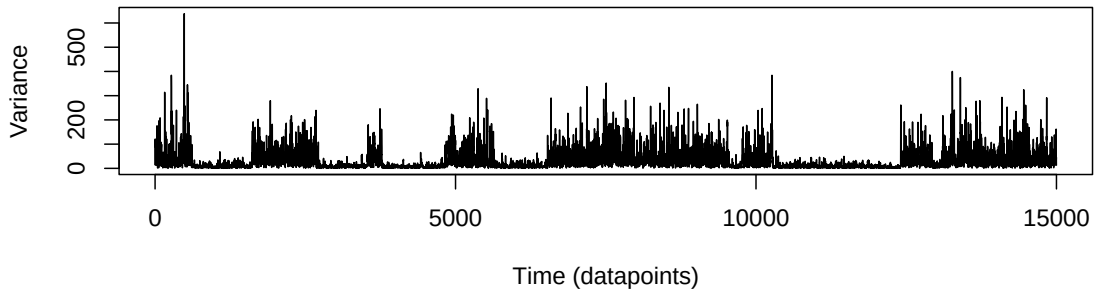

Figure 3.6. 1ms running variance transformation

We can then chunk out the the transition periods with our indices and apply changepoint analysis to each transition period that looked for the change in mean of the variance signal for every event and plot the results. The changepoint analysis looks for a change in mean of the variance signal. The analysis only looks for a single changepoint. *Note, this is an early version of the changepoint analysis that* ***lasertrapr*** *used. See the source code of the app on GitHub for up to date version.*

We can also plot the corresponding point in the raw/processed data that is ultimately used in the ensemble average:

This same approach can be applied to the backside. Once backside change points are identified than more precise measurements of time on, time off, displacements, and forces can be estimated. For now, we can go ahead and make one final plot showing the complete analysis overlayed on the raw/processed data. The pink shades indicates the start/end of the event. The vertical dashed lines are placed at the peak displacement of each event and labeled with the step size and event duration. No analysis is perfect, some shorter events are missed. These are usually running

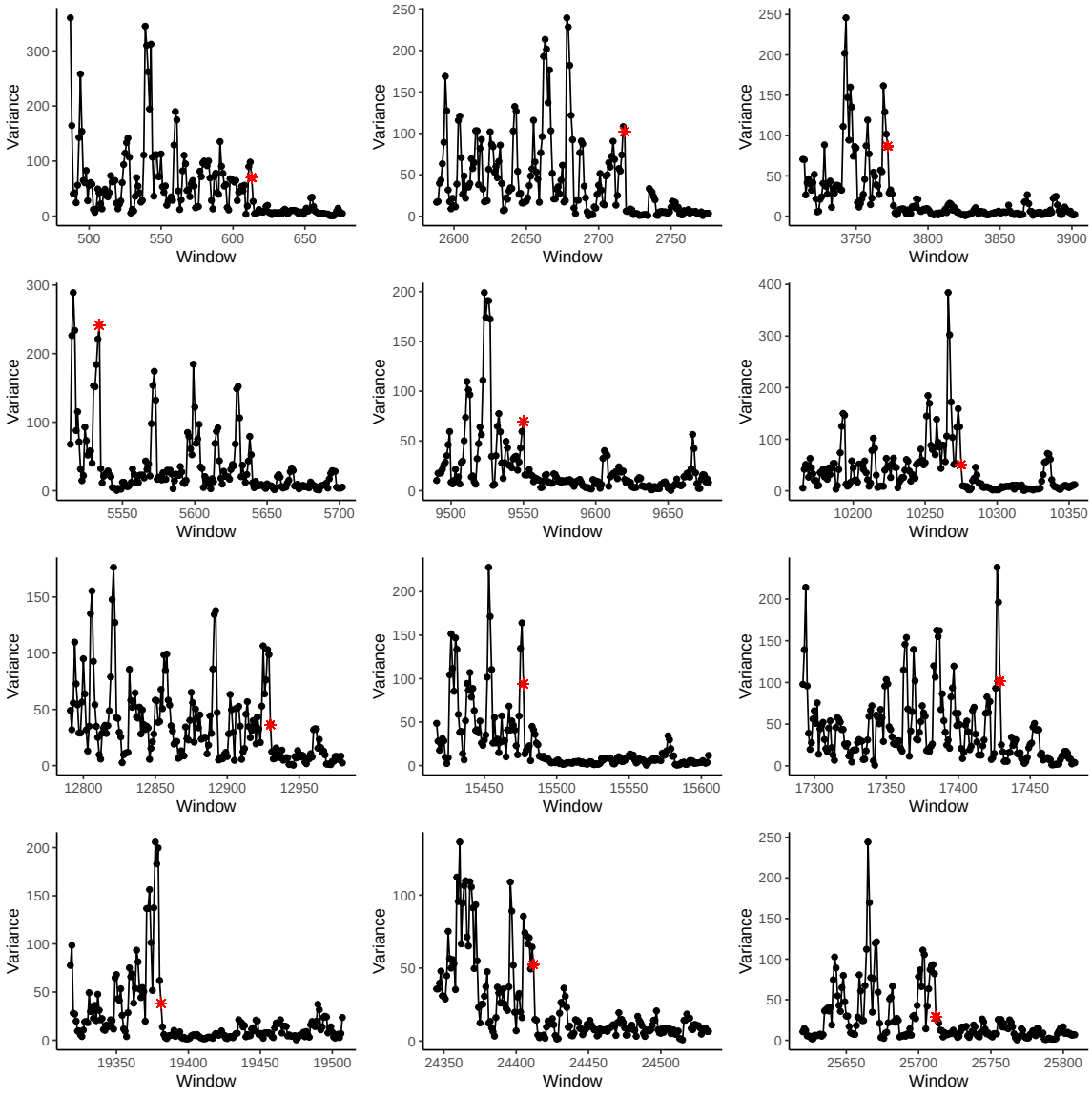

Figure 3.7. Changepoint identified start of event in running variance

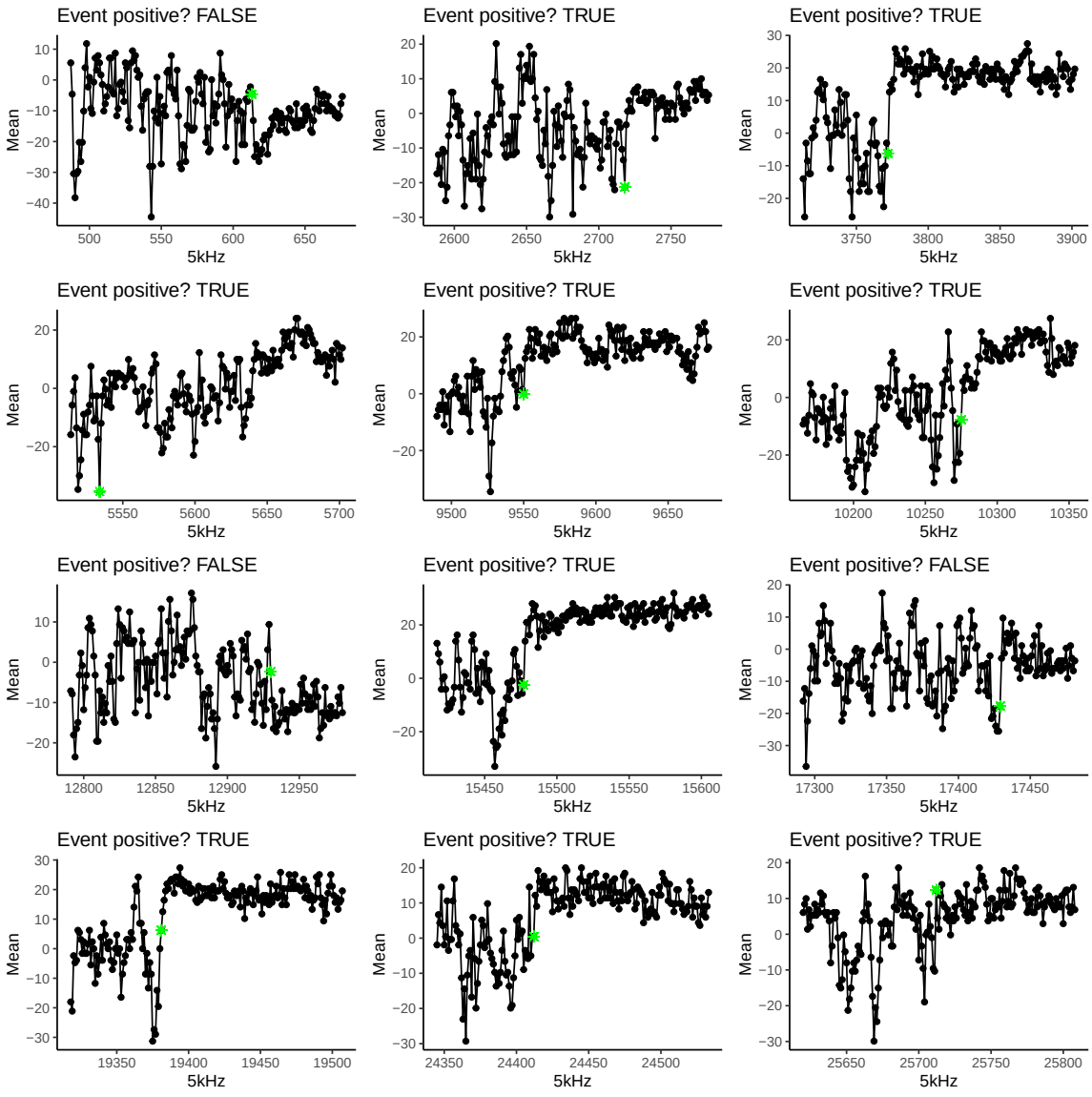

Figure 3.8. Changepoint identified start of event in the original data set

windows which have a high variance due to the window overlapping baseline and an event.

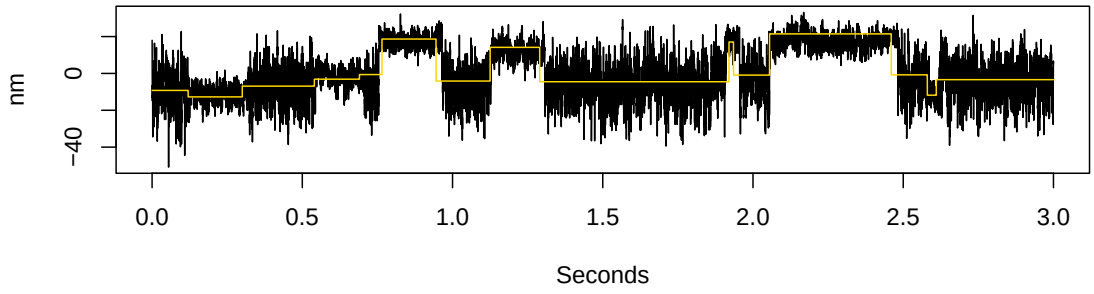

Figure 3.9. Results of analysis overlayed on data trace

BIBLIOGRAPHY

Ashkin, A., J. M. Dziedzic, J. E. Bjorkholm, and Steven Chu. 1986. "Observation of a Single-Beam Gradient Force Optical Trap for Dielectric Particles." *Optics Letters* 11 (5): 288–90. https://doi.org/10.1364/OL.11.000288.

Bailey, Kenneth. 1937. "Composition of the Myosins and Myogen of Skeletal Muscle." *Biochemical Journal* 31 (8): 1406–13.

Bassett, David R. 2002. "Scientific Contributions of A. V. Hill: Exercise Physiology Pioneer." *Journal of Applied Physiology* 93 (5): 1567–82. https://doi.org/10.1152/japplphysiol.01246.2001.

Blackwell, Thomas, W. Tom Stump, Sarah R. Clippinger, and Michael J. Greenberg. 2021. "Computational Tool for Ensemble Averaging of Single-Molecule Data." *Biophysical Journal* 120 (1): 10–20. https://doi.org/10.1016/j.bpj.2020.10.047.

Block, S M, and K Svoboda. 1995. "Analysis of High Resolution Recordings of Motor Movement." *Biophysical Journal* 68 (4 Suppl): 230S–241S.

Bloemink, Marieke J., and Michael A. Geeves. 2011. "Shaking the Myosin Family Tree: Biochemical Kinetics Defines Four Types of Myosin Motor." *Seminars in Cell & Developmental Biology*, Mechanochemical Cell Biology, 22 (9): 961–67. https://doi.org/10.1016/j.semcdb.2011.09.015.

Brandt, P W, R N Cox, M Kawai, and T Robinson. 1982. "Effect of Cross-Bridge Kinetics on Apparent Ca2+ Sensitivity." *Journal of General Physiology* 79 (6): 997–1016. https://doi.org/10.1085/jgp.79.6.997.

Capitanio, M., M. Canepari, P. Cacciafesta, V. Lombardi, R. Cicchi, M. Maffei, F. S. Pavone, and R. Bottinelli. 2006. "Two Independent Mechanical Events

in the Interaction Cycle of Skeletal Muscle Myosin with Actin." *Proceedings of the National Academy of Sciences* 103 (1): 87–92. https://doi.org/10.1073/pnas.0506830102.

Capitanio, Marco, Monica Canepari, Manuela Maffei, Diego Beneventi, Carina Monico, Francesco Vanzi, Roberto Bottinelli, and Francesco Saverio Pavone. 2012. "Ultrafast Force-Clamp Spectroscopy of Single Molecules Reveals Load Dependence of Myosin Working Stroke." *Nature Methods* 9 (10): 1013–19. https://doi.org/10.1038/nmeth.2152.

Cecchini, Marco, Yuri Alexeev, and Martin Karplus. 2010. "Pi Release from Myosin: A Simulation Analysis of Possible Pathways." *Structure* 18 (4): 458–70. https://doi.org/10.1016/j.str.2010.01.014.

Conibear, Paul B., Clive R. Bagshaw, Piotr G. Fajer, Mihály Kovács, and András Málnási-Csizmadia. 2003. "Myosin Cleft Movement and Its Coupling to Actomyosin Dissociation." *Nature Structural & Molecular Biology* 10 (10): 831–35. https://doi.org/10.1038/nsb986.

Dantzig, J. A., Y. E. Goldman, N. C. Millar, J. Lacktis, and E. Homsher. 1992. "Reversal of the Cross-Bridge Force-Generating Transition by Photogeneration of Phosphate in Rabbit Psoas Muscle Fibres." *The Journal of Physiology* 451 (1): 247–78. https://doi.org/10.1113/jphysiol.1992.sp019163.

Dominguez, Roberto, Yelena Freyzon, Kathleen M Trybus, and Carolyn Cohen. 1998. "Crystal Structure of a Vertebrate Smooth Muscle Myosin Motor Domain and Its Complex with the Essential Light Chain: Visualization of the PrePower Stroke State." *Cell* 94 (5): 559–71. https://doi.org/10.1016/S0092-8674(00)81598-6.

DUPUIS, D. E., W. H. GUILFORD, J. WU, and D. M. WARSHAW. 1997. "Actin Filament Mechanics in the Laser Trap." *Journal of Muscle Research & Cell Motility* 18 (1): 17–30. https://doi.org/10.1023/A:1018672631256.

Engelhardt, W. A., and M. N. Ljubimowa. 1939. "Myosine and Adenosinetriphosphatase." *Nature* 144 (3650): 668–69. https://doi.org/10.1038/144668b0.

Fenn, Wallace O. 1924. "The Relation Between the Work Performed and the Energy Liberated in Muscular Contraction." *The Journal of Physiology* 58 (6): 373–95. https://doi.org/10.1113/jphysiol.1924.sp002141.

Finer, Jeffrey T., Robert M. Simmons, and James A. Spudich. 1994. "Single Myosin Molecule Mechanics: Piconewton Forces and Nanometre Steps." *Nature* 368 (6467): 113–19. https://doi.org/10.1038/368113a0.

Forgacs, Eva, Takeshi Sakamoto, Suzanne Cartwright, Betty Belknap, Mihály Kovács, Judit Tóth, Martin R. Webb, James R. Sellers, and Howard D. White. 2009. "Switch 1 Mutation S217a Converts Myosin V into a Low Duty Ratio Motor." *The Journal of Biological Chemistry* 284 (4): 2138–49. https://doi.org/10.1074/jbc.M805530200.

Geeves, M. A., R. S. Goody, and H. Gutfreund. 1984. "Kinetics of Acto-S1 Interaction as a Guide to a Model for the Crossbridge Cycle." *Journal of Muscle Research and Cell Motility* 5 (4): 351–61. https://doi.org/10.1007/BF00818255.

Geeves, M. A., and K. C. Holmes. 1999. "Structural Mechanism of Muscle Contraction." *Annual Review of Biochemistry* 68: 687–728. https://doi.org/10.1146/annurev.biochem.68.1.687.

Gilson, M. K., T. P. Straatsma, J. A. McCammon, D. R. Ripoll, C. H. Faerman, P. H. Axelsen, I. Silman, and J. L. Sussman. 1994. "Open "Back Door" in a Molecular Dynamics Simulation of Acetylcholinesterase." *Science* 263 (5151): 1276–78. https://doi.org/10.1126/science.8122110.

Guilford, W. H., D. E. Dupuis, G. Kennedy, J. Wu, J. B. Patlak, and D. M. Warshaw. 1997. "Smooth Muscle and Skeletal Muscle Myosins Produce Similar Unitary Forces and Displacements in the Laser Trap." *Biophysical Journal* 72 (3): 1006–21. https://doi.org/10.1016/S0006-3495(97)78753-8.

Gulick, A. M., C. B. Bauer, J. B. Thoden, E. Pate, R. G. Yount, and I. Rayment. 2000. "X-Ray Structures of the Dictyostelium Discoideum Myosin Motor Domain with Six Non-Nucleotide Analogs." *The Journal of Biological Chemistry* 275 (1): 398–408. https://doi.org/10.1074/jbc.275.1.398.

Gunther, Laura K., John A. Rohde, Wanjian Tang, Joseph A. Cirilo, Christopher P. Marang, Brent D. Scott, David D. Thomas, Edward P. Debold, and Christopher M. Yengo. 2020. "FRET and Optical Trapping Reveal Mechanisms of Actin Activation of the Power Stroke and Phosphate Release in Myosin V." *Journal of Biological Chemistry* 295 (51): 17383–97. https://doi.org/10.1074/jbc.RA120.015632.

Gunther, Laura K., John A. Rohde, Wanjian Tang, Shane D. Walton, William C. Unrath, Darshan V. Trivedi, Joseph M. Muretta, David D. Thomas, and Christopher M. Yengo. 2019. "Converter Domain Mutations in Myosin Alter Structural Kinetics and Motor Function." *Journal of Biological Chemistry* 294 (5): 1554–67. https://doi.org/10.1074/jbc.RA118.006128.

Harris, D. E., and D. M. Warshaw. 1993. "Smooth and Skeletal Muscle Myosin Both Exhibit Low Duty Cycles at Zero Load in Vitro." *Journal of Biological Chemistry* 268 (20): 14764–68. https://doi.org/10.1016/S0021-9258(18)82398-5.

He, Zhen-He, Rod K. Chillingworth, Martin Brune, John E. T. Corrie, David R. Trentham, Martin R. Webb, and Michael A. Ferenczi. 1997. "ATPase Kinetics on Activation of Rabbit and Frog Permeabilized Isometric Muscle Fibres: A Real Time Phosphate Assay." *The Journal of Physiology* 501 (1): 125–48. https://doi.org/10.1111/j.1469-7793.1997.125bo.x.

Herzog, Walter, Krysta Powers, Kaleena Johnston, and Mike Duvall. 2015. "A New Paradigm for Muscle Contraction." *Frontiers in Physiology* 6. https://doi.org/10.3389/fphys.2015.00174.

Hill, A. V., and W. Hartree. 1920. "The Four Phases of Heat-Production of Muscle." *The Journal of Physiology* 54 (1-2): 84–128.

Hodge, Tony, M. Jamie, and T. V. Cope. 2000. "A Myosin Family Tree." *Journal of Cell Science* 113 (19): 3353–54. https://doi.org/10.1242/jcs.113.19.3353.

Holmes, Kenneth C., Isabel Angert, F. Jon Kull, Werner Jahn, and Rasmus R. Schröder. 2003. "Electron Cryo-Microscopy Shows How Strong Binding of Myosin to Actin Releases Nucleotide." *Nature* 425 (6956): 423–27. https://doi.org/10.1038/nature02005.

Houdusse, A., A. G. Szent-Györgyi, and C. Cohen. 2000. "Three Conformational States of Scallop Myosin S1." *Proceedings of the National Academy of Sciences* 97 (21): 11238–43. https://doi.org/10.1073/pnas.200376897.

Huxley, A. F., and R. Niedergerke. 1954. "Structural Changes in Muscle During Contraction: Interference Microscopy of Living Muscle Fibres." *Nature* 173 (4412): 971–73. https://doi.org/10.1038/173971a0.

HUXLEY, AF. 1957. "Muscle Structure and Theories of Contraction." *Prog. Biophys. Biophys. Chem* 7: 255–318.

Huxley, Hugh, and Jean Hanson. 1954. "Changes in the Cross-Striations of Muscle During Contraction and Stretch and Their Structural Interpretation." *Nature* 173 (4412): 973–76. https://doi.org/10.1038/173973a0.

Kitamura, Kazuo, Makio Tokunaga, Atsuko Hikikoshi Iwane, and Toshio Yanagida. 1999. "A Single Myosin Head Moves Along an Actin Filament with Regular Steps of 5.3 Nanometres." *Nature* 397 (6715): 129–34. https://doi.org/10.1038/16403.

Knight, Alex E., Claudia Veigel, Charles Chambers, and Justin E. Molloy. 2001. "Analysis of Single-Molecule Mechanical Recordings: Application to Acto-Myosin Interactions." *Progress in Biophysics and Molecular Biology*, Single Molecule Biochemistry and Molecular Biology, part II, 77 (1): 45–72. https://doi.org/10.1016/S0079-6107(01)00010-4.

Köhler, Jan, Gerhard Winkler, Imke Schulte, Tim Scholz, William McKenna, Bernhard Brenner, and Theresia Kraft. 2002. "Mutation of the Myosin Converter Domain Alters Cross-Bridge Elasticity." *Proceedings of the National Academy of Sciences of the United States of America* 99 (6): 3557–62. https://doi.org/10.1073/pnas.062415899.

König, Karsten. 2000. "Laser Tweezers and Multiphoton Microscopes in Life Sciences." *Histochemistry and Cell Biology* 114 (2): 79–92. https://doi.org/10.1007/s004180000179.

Llinas, Paola, Tatiana Isabet, Lin Song, Virginie Ropars, Bin Zong, Hannah Benisty, Serena Sirigu, et al. 2015. "How Actin Initiates the Motor Activity of Myosin." *Developmental Cell* 33 (4): 401–12. https://doi.org/10.1016/j.devcel.2015.03.025.

Longyear, Thomas, Sam Walcott, and Edward P. Debold. 2017. "The Molecular Basis of Thin Filament Activation: From Single Molecule to Muscle." *Scientific Reports* 7 (1): 1822. https://doi.org/10.1038/s41598-017-01604-8.

Lymn, R. W. 1974. "Actin Activation of Myosin ATPase," 43th series, 313–28.

Lymn, R. W., and E. W. Taylor. 1971. "Mechanism of Adenosine Triphosphate Hydrolysis by Actomyosin." *Biochemistry* 10 (25): 4617–24. https://doi.org/10.1021/bi00801a004.

Margossian, Sarkis S., and Susan Lowey. 1982. "[7] Preparation of Myosin and Its Subfragments from Rabbit Skeletal Muscle." In *Methods in Enzymology*, 85:55–71. Structural and Contractile Proteins Part B: The Contractile Apparatus and the Cytoskeleton. Academic Press. https://doi.org/10.1016/0076-6879(82)85009-X.

Mehta, A. D., J. T. Finer, and J. A. Spudich. 1997. "Detection of Single-Molecule Interactions Using Correlated Thermal Diffusion." *Proceedings of the National Academy of Sciences* 94 (15): 7927–31. https://doi.org/10.1073/pnas.94.15.7927.

Mentes, Ahmet, Andrew Huehn, Xueqi Liu, Adam Zwolak, Roberto Dominguez, Henry Shuman, E. Michael Ostap, and Charles V. Sindelar. 2018. "High-

Resolution Cryo-EM Structures of Actin-Bound Myosin States Reveal the Mechanism of Myosin Force Sensing." *Proceedings of the National Academy of Sciences* 115 (6): 1292–97.

Molloy, J. E., J. E. Burns, J. Kendrick-Jones, R. T. Tregear, and D. C. S. White. 1995a. "Movement and Force Produced by a Single Myosin Head." *Nature* 378 (6553): 209–12. https://doi.org/10.1038/378209a0.

Molloy, J E, J E Burns, J C Sparrow, R T Tregear, J Kendrick-Jones, and D C White. 1995b. "Single-Molecule Mechanics of Heavy Meromyosin and S1 Interacting with Rabbit or Drosophila Actins Using Optical Tweezers." *Biophysical Journal* 68 (4 Suppl): 298S–305S.

Muretta, Joseph M., John A. Rohde, Daniel O. Johnsrud, Sinziana Cornea, and David D. Thomas. 2015. "Direct Real-Time Detection of the Structural and Biochemical Events in the Myosin Power Stroke." *Proceedings of the National Academy of Sciences* 112 (46): 14272–77. https://doi.org/10.1073/pnas.1514859112.

Nesmelov, Yuri E., Roman V. Agafonov, Igor V. Negrashov, Sarah E. Blakely, Margaret A. Titus, and David D. Thomas. 2011. "Structural Kinetics of Myosin by Transient Time-Resolved FRET." *Proceedings of the National Academy of Sciences* 108 (5): 1891–96. https://doi.org/10.1073/pnas.1012320108.

Neuman, Keir C., and Attila Nagy. 2008. "Single-Molecule Force Spectroscopy: Optical Tweezers, Magnetic Tweezers and Atomic Force Microscopy." *Nature Methods* 5 (6): 491–505. https://doi.org/10.1038/nmeth.1218.

PAGE, E. S. 1954. "CONTINUOUS INSPECTION SCHEMES." *Biometrika* 41 (1-2): 100–115. https://doi.org/10.1093/biomet/41.1-2.100.

Pardee, J. D., and J. A. Spudich. 1982. "Purification of Muscle Actin." *Methods in Enzymology* 85 Pt B: 164–81. https://doi.org/10.1016/0076-6879(82)85020-9.

Patlak, J. 1993. "Measuring Kinetics of Complex Single Ion Channel Data Using Mean-Variance Histograms." *Biophysical Journal*. https://doi.org/10.1016/S0006-3495(93)81041-5.

Rayment, I., W. R. Rypniewski, K. Schmidt-Base, R. Smith, D. R. Tomchick, M. M. Benning, D. A. Winkelmann, G. Wesenberg, and H. M. Holden. 1993. "Three-Dimensional Structure of Myosin Subfragment-1: A Molecular Motor." *Science* 261 (5117): 50–58. https://doi.org/10.1126/science.8316857.

Reubold, Thomas F., Susanne Eschenburg, Andreas Becker, F. Jon Kull, and Dietmar J. Manstein. 2003. "A Structural Model for Actin-Induced Nucleotide Release in Myosin." *Nature Structural & Molecular Biology* 10 (10): 826–30. https://doi.org/10.1038/nsb987.

Robert-Paganin, Julien, Olena Pylypenko, Carlos Kikuti, H. Lee Sweeney, and Anne Houdusse. 2020. "Force Generation by Myosin Motors: A Structural Perspective." *Chemical Reviews* 120 (1): 5–35. https://doi.org/10.1021/acs.chemrev.9b00264.

Sellers, James R., and Claudia Veigel. 2010. "Direct Observation of the Myosin-Va Power Stroke and Its Reversal." *Nature Structural & Molecular Biology* 17 (5): 590–95. https://doi.org/10.1038/nsmb.1820.

Sleep, John, Malcolm Irving, and Kevin Burton. 2005. "The ATP Hydrolysis and Phosphate Release Steps Control the Time Course of Force Development in Rabbit Skeletal Muscle." *The Journal of Physiology* 563 (3): 671–87. https://doi.org/10.1113/jphysiol.2004.078873.

Smith, C. A., and I. Rayment. 1996. "X-Ray Structure of the Magnesium(II).ADP.vanadate Complex of the Dictyostelium Discoideum Myosin Motor Domain to 1.9 A Resolution." *Biochemistry* 35 (17): 5404–17. https://doi.org/10.1021/bi952633+.

Smith, David A., Walter Steffen, Robert M. Simmons, and John Sleep. 2001. "Hidden-Markov Methods for the Analysis of Single-Molecule Actomyosin

Displacement Data: The Variance-Hidden-Markov Method." *Biophysical Journal* 81 (5): 2795–2816. https://doi.org/10.1016/S0006-3495(01)75922-X.

Svoboda, K, and S M Block. 1994. "Biological Applications of Optical Forces." *Annual Review of Biophysics and Biomolecular Structure* 23 (1): 247–85. https://doi.org/10.1146/annurev.bb.23.060194.001335.

Sweeney, H. Lee, and Anne Houdusse. 2010. "Structural and Functional Insights into the Myosin Motor Mechanism." *Annual Review of Biophysics* 39 (1): 539–57. https://doi.org/10.1146/annurev.biophys.050708.133751.

Sweeney, H. Lee, Anne Houdusse, and Julien Robert-Paganin. 2020. "Myosin Structures." In *Myosins*, edited by Lynne M. Coluccio, 1239:7–19. Cham: Springer International Publishing. https://doi.org/10.1007/978-3-030-38062-5_2.

Tanaka, Hiroto, Akihiko Ishijima, Makoto Honda, Kiwamu Saito, and Toshio Yanagida. 1998. "Orientation Dependence of Displacements by a Single One-Headed Myosin Relative to the Actin Filament." *Biophysical Journal* 75 (4): 1886–94. https://doi.org/10.1016/S0006-3495(98)77629-5.

"The Nobel Prize in Physiology or Medicine 1922." n.d. *NobelPrize.org*. https://www.nobelprize.org/prizes/medicine/1922/summary/.

Trivedi, Darshan V., Joseph M. Muretta, Anja M. Swenson, Jonathon P. Davis, David D. Thomas, and Christopher M. Yengo. 2015. "Direct Measurements of the Coordination of Lever Arm Swing and the Catalytic Cycle in Myosin V." *Proceedings of the National Academy of Sciences* 112 (47): 14593–98. https://doi.org/10.1073/pnas.1517566112.

Trivedi, Darshan V., Joseph M. Muretta, Anja M. Swenson, David D. Thomas, and Christopher M. Yengo. 2013. "Magnesium Impacts Myosin V Motor Activity by Altering Key Conformational Changes in the Mechanochemical Cycle." *Biochemistry* 52 (27): 4710–22. https://doi.org/10.1021/bi4004364.

Trivedi, Darshan V., Suman Nag, Annamma Spudich, Kathleen M. Ruppel, and James A. Spudich. 2020. "The Myosin Family of Mechanoenzymes: From Mechanisms to Therapeutic Approaches." *Annual Review of Biochemistry* 89 (1): 667–93. https://doi.org/10.1146/annurev-biochem-011520-105234.

Tyska, M. J., D. E. Dupuis, W. H. Guilford, J. B. Patlak, G. S. Waller, K. M. Trybus, D. M. Warshaw, and S. Lowey. 1999. "Two Heads of Myosin Are Better Than One for Generating Force and Motion." *Proceedings of the National Academy of Sciences* 96 (8): 4402–7. https://doi.org/10.1073/pnas.96.8.4402.

Tyska, Matthew J., and David M. Warshaw. 2002. "The Myosin Power Stroke." *Cell Motility* 51 (1): 1–15. https://doi.org/10.1002/cm.10014.

Unger, Matthew, and Edward P. Debold. 2019. "Acidosis Decreases the Ca2+ Sensitivity of Thin Filaments by Preventing the First Actomyosin Interaction." *American Journal of Physiology-Cell Physiology* 317 (4): C714–18. https://doi.org/10.1152/ajpcell.00196.2019.

Veigel, Claudia, Marc L. Bartoo, David C. S. White, John C. Sparrow, and Justin E. Molloy. 1998. "The Stiffness of Rabbit Skeletal Actomyosin Cross-Bridges Determined with an Optical Tweezers Transducer." *Biophysical Journal* 75 (3): 1424–38. https://doi.org/10.1016/S0006-3495(98)74061-5.

Veigel, Claudia, Lynne M. Coluccio, James D. Jontes, John C. Sparrow, Ronald A. Milligan, and Justin E. Molloy. 1999. "The Motor Protein Myosin-I Produces Its Working Stroke in Two Steps." *Nature* 398 (6727): 530–33. https://doi.org/10.1038/19104.

Veigel, Claudia, Justin E. Molloy, Stephan Schmitz, and John Kendrick-Jones. 2003. "Load-Dependent Kinetics of Force Production by Smooth Muscle Myosin Measured with Optical Tweezers." *Nature Cell Biology* 5 (11): 980–86. https://doi.org/10.1038/ncb1060.

Veigel, Claudia, Fei Wang, Marc L. Bartoo, James R. Sellers, and Justin E. Molloy. 2002. "The Gated Gait of the Processive Molecular Motor, Myosin V." *Nature Cell Biology* 4 (1): 59–65. https://doi.org/10.1038/ncb732.

Walker, Matthew L., Stan A. Burgess, James R. Sellers, Fei Wang, John A. Hammer, John Trinick, and Peter J. Knight. 2000. "Two-Headed Binding of a Processive Myosin to F-Actin." *Nature* 405 (6788): 804–7. https://doi.org/10.1038/35015592.

Warshaw, David M., William H. Guilford, Yelena Freyzon, Elena Krementsova, Kimberly A. Palmiter, Mathew J. Tyska, Josh E. Baker, and Kathleen M. Trybus. 2000. "The Light Chain Binding Domain of Expressed Smooth Muscle Heavy Meromyosin Acts as a Mechanical Lever*." *Journal of Biological Chemistry* 275 (47): 37167–72. https://doi.org/10.1074/jbc.M006438200.

Woodward, Mike, Eric Ostrander, Seung P. Jeong, Xiarong Liu, Brent Scott, Matt Unger, Jianhan Chen, Dhandapani Venkataraman, and Edward P. Debold. 2020. "Positional Isomers of a Non-Nucleoside Substrate Differentially Affect Myosin Function." *Biophysical Journal* 119 (3): 567–80. https://doi.org/10.1016/j.bpj.2020.06.024.

Woody, Michael S, Donald A Winkelmann, Marco Capitanio, E Michael Ostap, and Yale E Goldman. 2019. "Single Molecule Mechanics Resolves the Earliest Events in Force Generation by Cardiac Myosin." Edited by Andrew P Carter, Olga Boudker, Michael Geeves, and Arne Gennerich. *eLife* 8 (September): e49266. https://doi.org/10.7554/eLife.49266.

Yount, R G, D Lawson, and I Rayment. 1995. "Is Myosin a "Back Door" Enzyme?" *Biophysical Journal* 68 (4 Suppl): 44S–49S.